
An interplay of Quantum Chaos and Quantum Channels

A thesis
submitted for the award of the degree of
Master of Science
in
Physics
by
Bidhi Vijaywargia
under the guidance of
Dr. Arul Lakshminarayan



**Department of Physics
Indian Institute of Technology Madras
Chennai 600036, India**

May 2023

CERTIFICATE

This is to certify that the project titled **An interplay of Quantum Chaos and Quantum Channels** is a bona fide record of work done by **Bidhi Vijaywargia** towards the partial fulfillment of the requirements of the Master of Science degree in Physics at the Indian Institute of Technology, Madras, Chennai 600036, India.

(Dr Arul Lakshminarayan, Project supervisor)

ACKNOWLEDGEMENTS

Foremost, I would like to express my sincere gratitude to my supervisor, Dr Arul Lakshminarayan for his guidance and supervision of my project. I am thankful to him for his support, patience and sharing his knowledge with me. I am also very grateful to him for his valuable time which he invested throughout the project. In addition to this, I would like to thank him for all his advice and I will always be indebted to him for all the knowledge I gained under his supervision.

I am thankful to Dr Ravi Prakash for his discussions on part of my project and for helping me tackle some of the problems. I am also thankful to Prof Vaibhav Madhok for providing me with some useful references. I would like to thank Abinash Sahu for some important discussions. I am also very grateful to my family for their constant support.

A big thanks to Ayanabha for his constant support and for always motivating me. He has been my greatest support system during the entire project. Thanks to Manishit and Tamojit for all their help both academic and non-academic and also Saurav, Mehraj, Kanan, and Snehil for their mental support and valuable advice. I am thankful to all my friends Ayanabha, Mehraj, Kanan, Manishit, Snehil, Tamojit, Saurav, Pratul, Dinesh, Lipsa and Sayak for their suggestions and emotional support.

ABSTRACT

We analyze a quantum channel corresponding to a quantum map that is interacting with an environment. We model one subsystem of a coupled quantum standard map as our system and the other as the environment. The standard map is a classical one dim non-autonomous system, the quantization of which is given by a unitary operator, U . In the first half, we review the relation between entanglement entropy of U and chaos for a coupled quantum standard map and also explore some *quantum signature of chaos*. In the later part, we study an open quantum standard map. The evolution of states for an open system is given by a quantum channel. We explore the spectral properties of the superoperator associated with the channel. The eigenvalue distribution lies on a unit circle in the case of no interaction, but as we increase the interaction, the eigenvalues start moving inside the unit circle in a way that goes from circular to annular. The extent of shrinking depends on the interaction strength and dimension of the system. The degeneracies in the eigenvalues are linked with the dynamics. As we move from regularity to chaos, the degeneracy in the eigenvalues decreases. Thus, in this work, we present some links between the spectral properties of the quantum channel for an open quantum dynamical map and the underlying classical dynamics associated with the map.

Contents

1	Introduction	1
1.1	A Bit of History	1
1.2	A Formal Definition of Chaos:	2
1.3	Motivations of the Thesis	3
1.4	A Link to Dual Unitary Circuits	4
1.5	Outline of the Thesis	8
2	Hamiltonian Chaos	9
2.1	Hamiltonian Systems	9
2.1.1	Integrable Systems	10
2.1.2	Non-Integrable Systems	11
2.1.3	KAM Theorem	11
2.1.4	Poincare-Birkhoff Theorem	12
2.2	Chaos in Hamiltonian Systems	12
2.3	Stroboscopic Maps	13
2.4	Kicked Hamiltonian Systems	15

2.4.1	Chirikov Standard Map	16
2.4.2	Salient Features of The Standard Map	17
2.5	Coupled Standard Map:	18
3	Preliminaries	21
3.1	Entanglement	21
3.2	Density Matrix and Reduced Density Matrix	22
3.3	Schmidt Decomposition	23
3.4	Von Neumann Entropy	24
4	Quantum Chaology	26
4.1	What is Quantum Chaos?	26
4.2	Quantum Maps	27
4.2.1	Quantum Standard Map	28
4.2.2	Quantization on Torus	29
4.2.3	Coherent States on the Torus	30
4.2.4	Quantum Map on Torus	31
4.2.5	Representing Quantum Standard Map on Torus	32
4.2.6	Coupled Quantum Standard Map	32
4.3	Relation Between Entanglement and Chaos	33
4.4	Numerical Results	34
4.4.1	Entanglement Entropy	34

4.4.2	Eigenstates and Reduced Density Matrix	36
5	Quantum Channels and Hamiltonian Systems	41
5.1	Quantum Channels	42
5.1.1	Completely Positive Trace Preserving Maps	42
5.1.2	Let's interact!	43
5.1.3	Operator-Sum Representation and Kraus Operators	44
5.1.4	Superoperator Representation	45
5.2	Quantum Channel for Hamiltonian Unitary	48
6	Spectral Properties of Quantum Dynamical Channels	49
6.1	Operator Entanglement	50
6.2	Norm of the channel, M	52
6.3	Spectral Properties	53
6.3.1	Relation between Eigenvalues, $\ M\ ^2$ and $E(U)$	53
6.3.2	Important features of channel and their impact on eigenvalue spectrum	55
6.3.3	Variation of eigenvalue distribution:	58
6.4	Relation Between Superoperator and Kraus Operators	67
7	Summary and Future work	72
A	Proof of Schmidt Decomposition	75
B	Derivation of Unitary, U for Quantum Standard Map	77

C Completely Positivity of Quantum Channel using Kraus Operators.	81
D Realignment and Partial Transpose Operation. Also deriving M and M_c	82

Chapter 1

Introduction

1.1 A Bit of History

Newton's laws allowed scientists to predict the motions of objects in simple, predictable systems, such as planets orbiting the sun. However, as scientists began to study more complex systems, such as the motion of fluids or the behaviour of gases, they found that the motion could become unpredictable and *chaotic*. Poincaré's in his work, "On the Problem of Three Bodies and the Equations of Dynamics." discovered that small changes in the initial conditions of the system could lead to vastly different outcomes, making long-term predictions of the behaviour of the system nearly impossible. However, it was not until the 1960s and 1970s that the field of "**chaos**" began to take shape as a distinct area of research.

On the other hand, in the early 20 century, quantum mechanics was being developed. Interesting and yet surprising behaviour which questioned our understanding of nature was observed. In the 1980s, physicists began to explore the relationship between quantum mechanics and chaos theory, leading to the introduction of "**Quantum Chaos**".

Classical physics provides an excellent description of many macroscopic systems. On the other hand, Quantum mechanics provides a more accurate description of microscopic systems, but it is still important to understand the limits of classical physics and how it emerges from quantum mechanics. So scientists tried to explore how chaos arises in the macroscopic limit. One of the key insights into quantum chaos was the discovery of the so-called "quan-

tum signature of chaos", which refers to the fact that the eigenspectra of a quantum system can reveal the underlying classical dynamics of the system[1].

Quantum mechanics and chaos theory both provide insights into the fundamental nature of the universe. By studying their relationship, one hopes to gain a deeper understanding of the underlying principles that govern the behaviour of matter and energy at the smallest scales.

1.2 A Formal Definition of Chaos:

There is no universal definition of chaos, but we present a definition used by Devaney in his textbook[2]. If we consider a continuous map, $f: \Omega \rightarrow \Omega$ where Ω is the phase space when f corresponds to a dynamical map, then the map is said to be chaotic if it has the following three properties:

- **Transitivity:** If we consider non-empty open subsets, A and B of Ω , then after some integer n , $f^n(A) \cap B$ will be non-empty. This means that after n iterations of the dynamical map, the points under iterations will move from one arbitrarily small neighbourhood to another.
- **Dense set of periodic orbits:** It means that arbitrarily close to any point there is a periodic orbit or in other words if we choose a closed interval close to any point in Ω we can find a periodic orbit in that interval.
- **Sensitive Dependence of initial conditions:** The dynamical map, f is such that if we consider two points, x in Ω and y in the neighbourhood of x , separated by a positive real number, δ_0 then, after n iterations of the map, f , the separation between them is greater than δ_0 , i.e., $|f^n(x) - f^n(y)| > \delta$ where, $\delta = |x - y|$.

For chaotic systems, the sensitive dependence implies exponential divergence of trajectories. after some transient time and the rate is given by a quantity known as Lyapunov of Exponent. The Lyapunov of exponent is defined below[3].

Let us take two points in the phase space, Ω separated x_0 and y_0 separated by a distance, δ_0 . Let x_n and y_n denote the evolution of x and y after n^{th} iteration of the dynamical map, f . The distance between the x_n and y_n is now, δ_n . The Lyapunov of exponent for the initial point x_0 is then defined as -

$$\lambda = \lim_{n \rightarrow \infty} \lim_{\delta_0 \rightarrow 0} \frac{1}{n} \log \frac{\delta_n}{\delta_0} \quad (1.1)$$

A system with a positive value of λ along with transitivity and a dense set of periodic orbits is known as a **chaotic system**. The exponential divergence should not be forever and that is why we require bounded phase space.

In principle, chaotic behaviour is not random and it appears even in deterministic systems which makes it different from noise. That is why one usually refers to it as '**Deterministic Chaos**'. Some deterministic systems which exhibit chaos are the double pendulum, Lorenz map and even the motion of planets in the solar system.

1.3 Motivations of the Thesis

Everything interacts with everything!

One of the basic assumptions which we make is that the system is isolated and does not interact with the surrounding. However, at times we need to lift this assumption. The evolution of the state of an isolated quantum system is given by Schrodinger's equation of motion. As a consequence of this, evolution is always unitary for an isolated system. But, this no longer holds if we consider the interaction of the quantum system with the environment which cannot be ignored in practical purposes. Such systems are known as open systems and the evolution of an open system is no longer unitary. However, we can now rely on another quantum operation which now gives the evolution of the states in an open quantum system. These evolutions are a special kind of quantum operation/channel known as a completely positive and trace-preserving map. The evolution of the system and environment is still unitary as they together form an isolated system. The channel can be represented by a superoperator.

The unitary, U determines the form of the channel for the system alone. As we are interested in chaos, the unitary which we choose corresponds to the quantum standard map which is the quantization of the classical standard map, which shows a transition to chaos. We were interested in finding the link between the underlying dynamics(regularity and chaos) on the quantum channel. With this motivation, we explored the spectral properties of the quantum channel associated with a dynamical quantum map.

1.4 A Link to Dual Unitary Circuits

An alternative theoretical arena for studying many-body quantum dynamics is provided by random unitary circuits, which offer ways to obtain analytic outcomes outside the scope of regularity, i.e., Models of non-integrable many-body quantum systems using random unitary circuits are being extensively studied. Of special interest to us are dual-unitary circuits.

A unitary operator, U can be represented diagrammatically as shown in Ref.[4], by Fig.1.1. For a bipartite unitary operator, U which lives in Hilbert space, $\mathcal{H}^d \otimes \mathcal{H}^d$ where d is the local dimension, the diagrammatic representation of U is given as - The relation $UU^\dagger = I$ can then

$$\langle i\alpha | U | j\beta \rangle = \begin{array}{c} i \\ \diagdown \\ \text{[teal square]} \\ \diagup \\ j \end{array} \quad , \quad U^\dagger = \begin{array}{c} \alpha \\ \diagup \\ \text{[red square]} \\ \diagdown \\ \beta \end{array} .$$

Figure 1.1: A diagrammatic representation of a bipartite unitary, U . This figure is taken from [5]

be represented by connecting the legs, which is equivalent to contracting two indices as -

$$\begin{array}{c} i \\ \diagdown \\ \text{[teal square]} \\ \diagup \\ j \end{array} \quad = \quad \left. \begin{array}{c} i \\ \diagup \\ \text{[red square]} \\ \diagdown \\ j \end{array} \right\} \quad , \quad U^\dagger U = \mathbb{1} \equiv \left(\begin{array}{c} \alpha \\ \diagup \\ \text{[red square]} \\ \diagdown \\ \beta \end{array} \right) \left. \right\} .$$

Figure 1.2: An diagrammatic representation of identity for a unitary operator, U . This figure is taken from [5]

Circuits when built using a special type of unitary, U which is dual are known as dual-unitary circuits, as shown in Ref [4]. What do we mean by unitary operator being dual? A unitary operator is dual when reshuffling of the Unitary, U is also unitary. In particular, U^{R_2} is also unitary, where R_2 is realignment operation discussed in Appendix D. Identity can then also be expressed as shown in Fig.1.3

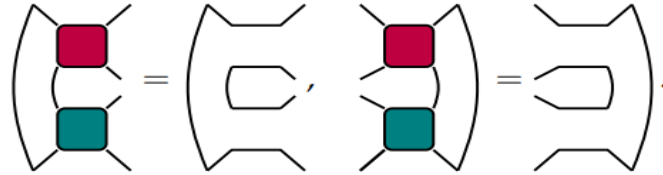


Figure 1.3: An representation of Identity when U is dual unitary. This figure is taken from [5]

We can now consider a chain of particles and each particle is also referred to as a site. The bipartite unitary, U is then acted on two neighbouring sites and one can repeat it any number of times, as shown in fig 1.4 for eight particles and two-time steps. In Fig.1.4, the bottom

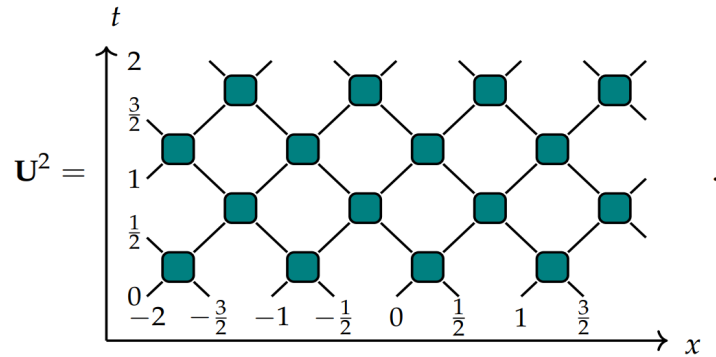


Figure 1.4: Two time steps of a Floquet operator, \mathbf{U} in terms of a dual unitary circuit. This figure is taken from [5]

$$\mathbf{U} = \mathbf{T}_{2L} U^{\otimes L} \mathbf{T}_{2L}^\dagger U^{\otimes L}$$

Figure 1.5: The Floquet operator, U as given in [5].

two arrays correspond to one time step of the Floquet operator, \mathbf{U} and on repetition of the

bottom array we get \mathbf{U}^2 for two-time steps. We can do it for t times and this will give the time-evolution operator, \mathbf{U}^t for the dynamic for t time steps. In fig.1.5, U is the bipartite unitary acting on the neighbouring particles, and corresponding to eight particles, and L is four for Fig. 1.4 and $\mathbf{T}_{2L}|k_1\rangle \otimes |k_2\rangle \otimes \dots \otimes |k_{2L}\rangle = |k_2\rangle \otimes |k_3\rangle \otimes \dots \otimes |k_{2L}\rangle \otimes |k_1\rangle$ is the site translation operator.

Dual unitary circuits were introduced by Bertini, Kos and Prosen [4], which provided a tool for developing an ergodic theory of quantum many-body. A brief summary and some key results of the work are presented below. In classical many-body systems, the behaviour of

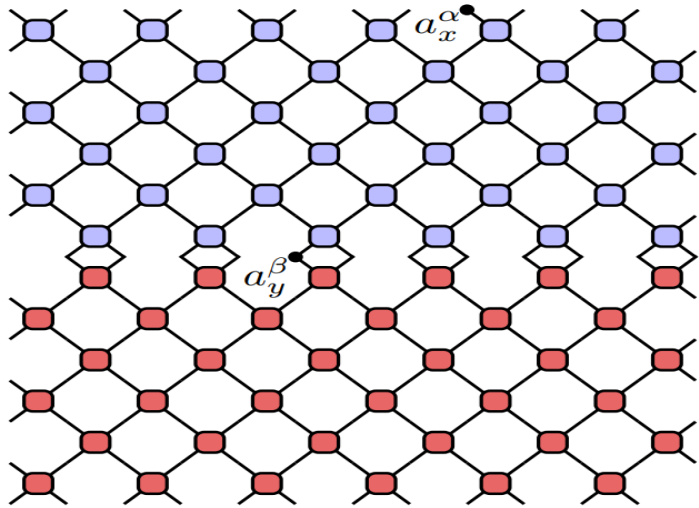


Figure 1.6: A dual unitary circuit representation of a floquet operator, U . The a_y^β and a_x^α are some local observables at site y and x respectively and time β and α respectively. This is taken from ref [4].

local interactions can be described by the correlation functions between two local observables at different space-time coordinates. The correlation functions can then characterise the ergodic properties of the classical many-body system. In particular, the decay of correlation functions is related to ergodic or mixing behaviour. In the quantum many-body locally interacting systems it is difficult to find the decay of correlations functions.

In this work, the authors have used dual unitary circuits to develop an ergodic theory of quantum many-body systems in a similar sense as classical ergodic theory, i.e., via decay of spatiotemporal correlation functions. They have used the circuit as illustrated in Fig. 1.6. Here, the horizontal direction is space and the vertical direction is time.

The work is pivoted at finding the spread of local observable, a_y^β after the time step, say t . This has been characterized by finding the correlation function between a_y^β and a_x^α where, x and α are varied over all the sites. They got a non-zero value of these correlation functions as defined in Ref [4] only on the lightcone as represented in Fig. 1.7 The main result that

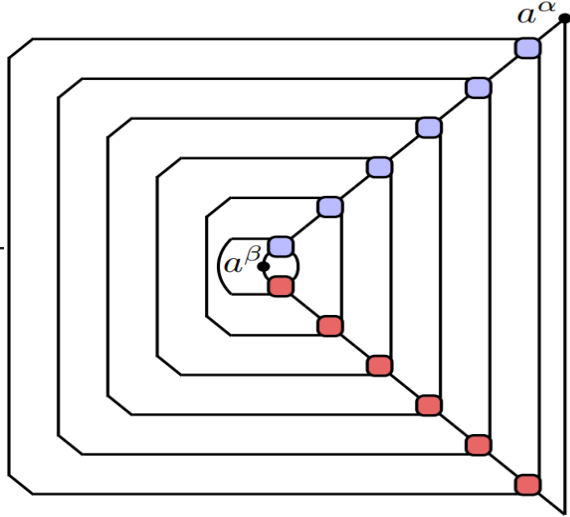


Figure 1.7: The circuit representing that the correlation functions vanishes only along the light cone. This is taken from ref [4].

interests us is the following. It has been presented in the paper that all local correlations in dual unitary circuits are determined by quantum channels corresponding to just the bipartite unitary, $U(d^2 \times d^2)$ acting on the two neighbouring sites. These channels are Completely positive, trace-preserving and unital. The diagrammatic representation of these channels is given in Fig. 1.8.

It has been shown that the decay of correlation functions is then determined by the eigenvalues of these channels, which lie inside a unit disk. The spectral properties of the channel then give a way to classify dual unitary circuits on the basis of ergodic properties of local unitary observables as presented in Ref [4] and [5]. These results can motivate us to look at the spectral properties of a quantum channel corresponding to bipartite Unitary, U . The unitary we take is not random but corresponds to the coupled quantum standard map, which shows a transition from regularity to chaos.

$$\mathcal{M}_+(a) = \frac{1}{q} \text{tr}_1 \left[U^\dagger (a \otimes \mathbb{1}) U \right] = \frac{1}{q} \left(\begin{array}{c} \text{red square} \\ a \bullet \\ \text{teal square} \end{array} \right),$$

$$\mathcal{M}_-(a) = \frac{1}{q} \text{tr}_2 \left[U^\dagger (\mathbb{1} \otimes a) U \right] = \frac{1}{q} \left(\begin{array}{c} \text{red square} \\ \bullet a \\ \text{teal square} \end{array} \right).$$

Figure 1.8: A diagrammatic representation of a quantum channel associated with the bipartite unitary, U . This is taken from ref[4].

1.5 Outline of the Thesis

The thesis is divided into 7 chapters. As most of the work is based on Quantum Chaos, one needs a foundational knowledge of hamiltonian chaos which is discussed in Chapter 2. Chapter 3 includes some basic definitions before we move to quantum chaos. After getting a brief understanding of hamiltonian chaos, we understand quantum chaos using a classical dynamical map, standard Map and also various quantum signatures of chaos on entanglement as presented in Chapter 4. The rest of the thesis is focused on Quantum Channels, which is the main part of this work. In Chapter 5, we discuss what a quantum channel is and finally, in Chapter 6, we present our results on the study of the spectral properties of the Quantum Channel. In the end, we summarize the thesis and talk about future work in chapter 7.

Chapter 2

Hamiltonian Chaos

Classical mechanics deals with the motion of objects under the influence of forces, and it has been highly successful in explaining the behaviour of macroscopic objects, including the movement of planets in the solar system. However, when constraints are present, it is more convenient to use generalized coordinates, which then define the configuration of the system in terms of the degrees of freedom allowed by the constraints. The Lagrangian and Hamiltonian formulations of classical mechanics provide a robust framework for describing the dynamics of a system in terms of its generalized coordinates. In the Lagrangian formulation, the dynamics are characterized by the Lagrangian, a function of the generalized coordinates and their time derivatives.

In the Hamiltonian formulation, the dynamics are indicated by the Hamiltonian, a function of the generalized coordinates and their conjugate momenta. Both the Lagrangian and Hamiltonian formulations of classical mechanics are powerful tools for analyzing the dynamics of various physical systems, from simple pendulums to complex mechanical systems and beyond.

2.1 Hamiltonian Systems

Hamiltonian formalism plays a vital role in modern classical, statistical, and quantum mechanics. We use sets of first-order differential equations to describe the motion.

If n is the number of degrees of freedom, then we have, $\{q_1, q_2, \dots, q_n\}$, generalized coordinate and n -corresponding conjugate momenta, p_i 's. This gives $2n$ independent variables, which forms a $2n$ dim phase space. In this $2n$ dim phase space, the trajectory gives the system's motion. The time evolution of the phase space variable is then given by-

$$\frac{d\mathbf{q}}{dt} = \frac{\partial H(p, q, t)}{\partial \mathbf{p}} \quad (2.1.a)$$

$$\frac{d\mathbf{p}}{dt} = -\frac{\partial H(p, q, t)}{\partial \mathbf{q}} \quad (2.1.b)$$

Here, $\mathbf{q}=\{q_1, q_2, \dots, q_n\}$ and $\mathbf{p}=\{p_1, p_2, \dots, p_n\}$. $H(p, q, t)$ is the hamiltonian of the system.

The above equations are known as Hamilton's equation of motion. If, for a system, the above set of equations is satisfied, then such systems are called Hamiltonian Systems. For systems in which Hamiltonian is the function of time, t is called non-autonomous, and for time-independent cases, it is called an autonomous system. It is important to note that Hamiltonian systems preserve the volume of the phase space.

2.1.1 Integrable Systems

Let us consider the case of an autonomous system. For such cases, the Hamiltonian, H can be identified as energy and is a constant of motion¹. The formal definition of integrability is given by Liouville and Arnold as-

"For a Hamiltonian system with n degrees of freedom, if there exist n independent constants of motion, $C_i(\mathbf{q}, \mathbf{p})$, $\{i=1, 2, \dots, n\}$ which are in mutual involution, i.e., $\{C_i, C_j\} = 0$ then, such Hamiltonian systems are said to be integrable."

Here, $\{C_i, C_j\}$ denotes the Poisson bracket between C_i and C_j and it is defined as -

$$\{C_i, C_j\} = \sum_{i=1}^n \frac{\partial C_i}{\partial q_i} \frac{\partial C_j}{\partial p_i} - \frac{\partial C_j}{\partial q_i} \frac{\partial C_i}{\partial p_i} \quad (2.2)$$

Also, if the system is integrable, then there exists a canonical transformation from (q_i, p_i) to action-angle variable (θ_i, I_i) , such that the Hamiltonian in terms of the new variable is only

¹If an observable F doesn't depend on time and $\{F, H\} = 0$, then F is a constant of motion.

dependent on I_i 's, which are functions of C_i 's. The phase space is then confined on an n-dim Torus[6]. For the case of n=2, the torus has a similar structure to a "Vada". In this case, we have two angles, $\{\theta_1, \theta_2\}$ which are related to frequency, $\{\omega_1, \omega_2\}$ and $\omega_i = \omega_i(I_1, I_2)$. The ratio of frequency, $r = \omega_1/\omega_2$ can be rational or irrational. When r is a rational number, we get a periodic orbit and such tori are called resonant tori. In contrast, when r is irrational, we get a quasi-periodic orbit². Tori, in this case, is called a non-resonant tori.

2.1.2 Non-Integrable Systems

A 1-d autonomous system is always integrable as energy is a constant of motion. But, as we move to two or higher degrees of freedom(dof's), we might not have enough constants of motion. The Hamiltonian system is then said to be non-integrable. There are exceptional cases for $n \geq 2$ where we can find enough constants of motion to ensure integrability, but such systems are scarce, i.e., of measure zero—for example- central force problem, uncoupled non-linear oscillators. Thus, in most cases, we would have to deal with non-integrable systems. For non-autonomous systems, even a 1-dof system can be non-integrable as energy is no longer a constant of motion.

2.1.3 KAM Theorem

KAM theorem, named after mathematicians Kolmogorov, Arnold, and Moser, is a fundamental result in classical mechanics that explains the persistence of quasi-periodic motion in Hamiltonian systems subjected to small perturbations. In particular, the KAM theorem states that for a large class of Hamiltonian systems, if the system has a certain amount of invariant tori (which represent quasi-periodic motion), then small perturbations to the system will preserve the tori and lead to quasi-periodic motion of the perturbed system. This means that the system will not necessarily become chaotic, but instead, the quasi-periodic motion will persist despite the perturbations. The KAM theorem is essential because it provides a framework for understanding the behaviour of Hamiltonian systems under perturbations.

²The trajectories never close on themselves, but it passes close to every point on the torus. Hence, the trajectory densely covers the torus. However, the orbit is still bounded and confined on the torus but not closed.

It has applications in many areas of physics, such as in the study of celestial mechanics, plasma physics, and condensed matter physics.

2.1.4 Poincare-Birkhoff Theorem

The theorem deals with the fate of resonant tori in the presence of perturbation. This theorem says that when we slightly perturb the integrable Hamiltonian to get non-integrability, the rational, also known as resonant tori, breaks up into alternating sequences of elliptic and hyperbolic points. Each elliptical point will be surrounded by elliptical orbits.

2.2 Chaos in Hamiltonian Systems

We have stated that autonomous systems with one dof are always integrable and thus cannot have chaotic motions for any initial conditions. But, this no longer holds when our Hamiltonian explicitly depends on time. Thus, we can have chaos even for non-autonomous systems with one dof. Such systems are also referred to as 1.5 dof systems, as time can be considered as another variable. We restrict ourselves to 1 dof the non-autonomous Hamiltonian systems to observe the behaviour of trajectories in the presence of Chaos. An easier way to study this is by forcing an integrable one dof system.

Consider the following example of a parametrically forced harmonic oscillator and pendulum[7]. Hamiltonian for the two cases is given as-

$$H_h = \frac{p^2}{2} + g_0(1 + \epsilon \sin(2\pi t)) \frac{q^2}{2} \quad (2.3)$$

$$H_p = \frac{p^2}{2} + g_0(1 + \epsilon \sin(2\pi t))(1 - \cos q) \quad (2.4)$$

here, $g_0\epsilon$ = amplitude of force, the period of the forcing is one. And, $\epsilon = 0$ is the case of no forcing, and it represents the autonomous system.

Using Hamilton's equation of motion, we get,

$$\frac{dq}{dt} = p; \frac{dp}{dt} = -g_0(1 + \epsilon \sin(2\pi t))q \quad (2.5)$$

$$\frac{dq}{dt} = p; \quad \frac{dp}{dt} = -g_0(1 + \epsilon \sin(2\pi t)) \sin(q) \quad (2.6)$$

where eq.2.5 is for forced harmonic oscillator and eq.2.6 if for forced pendulum.

The solution of the above equation gives the trajectory in the phase space for that initial condition. We then look at two initial points which are close to each other for both cases as illustrated in fig.2.1. From Fig. 2.1, the trajectories appear to cross, but this is not the case

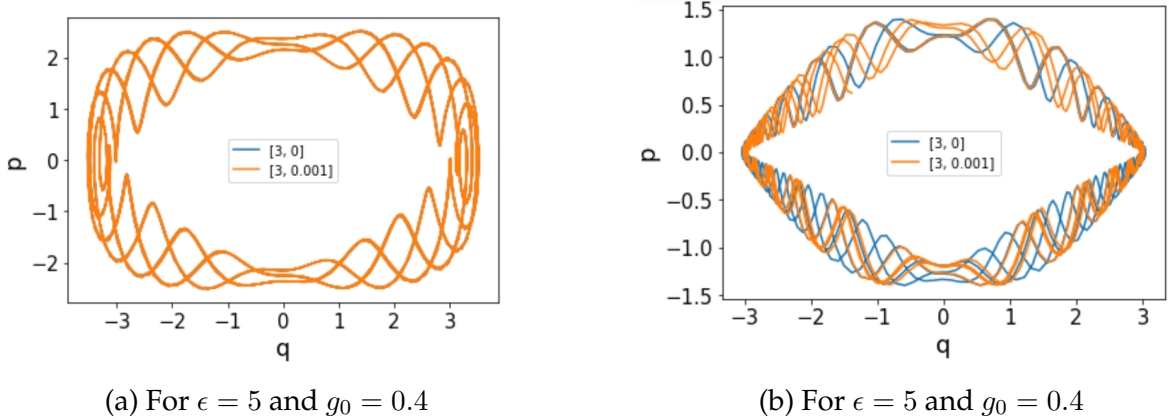


Figure 2.1: The phase-space of parametrically forced harmonic oscillator and pendulum. Here we show two trajectories starting at nearby points. $(q_0, p_0) = (3,0)$ for orange and $(3,0.001)$ for blue trajectory. In the case of the forced harmonic oscillator, the two coincide. However, for the forced pendulum case, we get two distinct trajectories.

as we also have time as a variable now, and two trajectories can cross at different times, t . In the case of the parametrically forced harmonic oscillator, we cannot distinguish between the two trajectories corresponding to the two nearby initial conditions. However, in the case of a parametrically forced pendulum, the two trajectories become distinct. Thus, there is sensitive dependence on the initial conditions. Sensitive dependence on the initial condition is an important feature of chaotic motions, but it does not guarantee chaos.

2.3 Stroboscopic Maps

We can reduce flows to maps by the Poincaré surface of section technique[8]. So far, we have been treating time as a continuous variable. But, we can also discretize time and look at the phase space variables at discrete times. This is one way to get the Poincaré surface. Before

talking more about it, we should address the question of **why maps?**

Fig. 2.1 is for two trajectories. But, what if we want to observe many trajectories together? If we include more trajectories, the behaviour can be complicated for flows. This problem is solved to some extent if we move to maps. We would like to focus on systems with periodic forcing. In such cases, we can look at the phase space at discrete times with intervals equal to the period of forcing. So, we get to see where a point maps after one time period. This is known as **Stroboscopic Map.**,[7],[9]-[10].

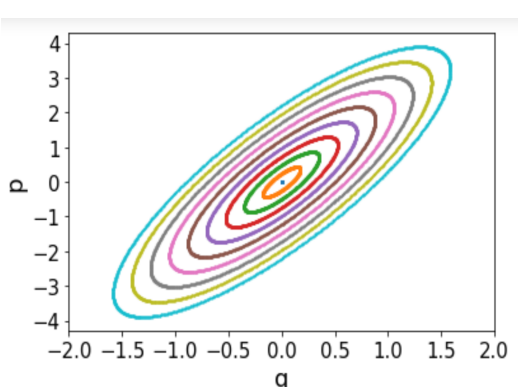
Let us consider the form of Hamiltonian [7] as-

$$H(q, p, t) = f(p) + g(t)V(q) \quad (2.7)$$

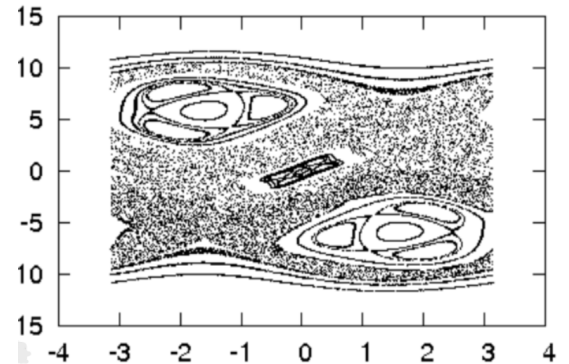
here, $g(t)$ =forcing and f and V are some functions³. Now, consider that $g(t)$ is periodic with some period T , then -

$$H(t) = H(t + T) \quad (2.8)$$

Thus, we can look at (q, p) at the integer multiple of T to get the map⁴. For a parametrically forced harmonic oscillator, the stroboscopic map is given in Fig 2.2 (a) and for the parametrically forced pendulum in fig.2.2(b). We can see phase space for the forced harmonic



(a) Forced harmonic oscillator.



(b) Forced simple pendulum. This figure is taken from Ref.[7]

Figure 2.2: The stroboscopic map for a forced harmonic oscillator and forced pendulum with forcing parameters $\epsilon=10$ and $g_0=1$. It shows many initial conditions iterated over 10000-time steps.

oscillators is filled with elliptical orbits⁵.On the contrary, for a forced pendulum, the points

³For the case SHO and simple pendulum, $f=\frac{p^2}{2}$ and $V = \frac{q^2}{2}$ and $V = (1 - \cos q)$ respectively.

⁴Equation 2.8 is not always true. It holds only when $g(t)$ is periodic.

⁵Note that this is not an orbit but the value of phase space variables at discrete times, with intervals equal to the period of forcing function.

are randomly scattered over the entire phase space, but there are few periodic islands. This random scatter of points corresponds to chaotic motion. Such a phase space is known as a mixed phase space, where we have a mixture of both chaos and regularity.

Stroboscopic map for a system has the form -

$$q_{n+1} = f(q_n, p_n); \quad p_{n+1} = g(q_n, p_n) \quad (2.9)$$

The features in the phase space of flow get faithfully carried onto maps. Since it is easier to study maps, most of my thesis will be related to maps.

2.4 Kicked Hamiltonian Systems

The situation is not as simple as we thought it would be if move to maps! We can always go from a flow to a map, but in general writing, the explicit forms of the function, f and g (defined in equation 2.9) are obscure⁶. However, we still have some success in writing the non-linear stroboscopic map when the forcing is a train of the Dirac-delta function. The forcing is, thus, impulsive and is at regular time intervals which is the period of forcing. Systems of these kinds are often referred to as Kicked Hamiltonian Systems.

The form of the Hamiltonian for such systems is then given by-

$$H = f(p) + \sum_{n=-\infty}^{\infty} \delta(t/T - n)V(q) \quad (2.10)$$

Using this we get Hamilton's EOM as -

$$\frac{dq}{dt} = f'(p) \quad (2.11.a)$$

$$\frac{dp}{dt} = - \sum_{n=-\infty}^{\infty} \delta(t/T - n)V'(q) \quad (2.11.b)$$

From these two equations, we can say that in between the kicks, the momentum is constant and the position changes. At the kicks, we can assume the position to be frozen and the

⁶For SHO, we can write a linear stroboscopic map explained in ref [7]

momentum to be changing due to the nature of the Dirac-delta function. Integrating the above equation at one time period T , we get the following stroboscopic map -

$$q_{n+1} = q_n + Tf'(p_n) \quad (2.12.a)$$

$$p_{n+1} = p_n - TV'(q_{n+1}) \quad (2.12.b)$$

Here, q_n and p_n denote the position and momentum just after the n^{th} kick. The map then relates the value of position and momentum just after n^{th} and $(n + 1)^{th}$ kick.

2.4.1 Chirikov Standard Map

The stroboscopic map, in the case, when the system is a pendulum that is being kicked periodically, is known as Standard Map. It is also known as Chirikov-Taylor Map or Kicked Rotor (or Rotator). For kicked pendulum, $f(p)$ and $V(q)$ has the form -

$$f(p) = \frac{p^2}{2} \quad (2.13.a)$$

$$V(q) = -g \frac{\cos(2\pi q)}{(2\pi)^2} \quad (2.13.b)$$

The map is then, given by

$$q_{n+1} = q_n + p_n \pmod{1} \quad (2.14.a)$$

$$p_{n+1} = p_n - \frac{K}{2\pi} \sin(2\pi q_{n+1}) \pmod{1} \quad (2.14.b)$$

We have rescaled momentum as $Tp \rightarrow p$ and $K = Tg$. Modulo one operation is done to make the phase space square of unit length. However, natural phase space is a cylinder and is cyclic along q . q is an angle, so, we can take the modulo 2π operation. But for momentum, this is possible only because the standard map is invariant under the translation of momentum by an integer multiple of 2π . So, the phase space is now a square of length 2π , which we have rescaled down to a square of unit length. Here, we have one parameter, K , which controls the dynamics of the system, as we shall see. It is known as the control parameter.

The physical system corresponding to the Standard Map is a simple pendulum that is free to rotate around its axis and the tip of which is being kicked periodically. The relation between

the position and momentum of the pendulum just after n^{th} and just after the $(n + 1)^{th}$ kick is then given by equation 2.12. The constant K is then proportional to the strength of the kicking on the rotor. Many physical systems in mechanics, accelerator, plasma and solid-state physics can be approximated to Kicked Rotor. Also, this map plays an important role in studying Hamiltonian chaos. It is a conservative system displaying chaotic behaviour which was first established by Chirikov in 1969, [11]-[12]. It is easy to get the quantized version of this map, and one can get more insight into quantum chaos, as we shall see in the subsequent chapters.

2.4.2 Salient Features of The Standard Map

- **Phase-space Plots:**

The phase space plots as we vary the intensity of kicking, which is given by K , are given in Fig. 2.3. We can see that as we vary K , we go from regular to chaotic motion. It is interesting to see chaotic behaviour in the phase space of a low-dimensional Hamiltonian system. The parameter K is called the control parameter. We can see for large K , we still have few unstable periodic orbits. Periodic orbits are dense, but they are of measure zero.

- **Fate of resonant and non-resonant curves:**

When $K = 0$, we have integrability and trajectories are nothing but straight lines of constant momentum. We have two kinds of trajectories, resonant and non-resonant. For resonant trajectories, p is rational and irrational for non-resonant trajectories. When p is irrational say, p_0 then a single orbit densely fills the line $p = p_0$. Now, as we increase K slightly(only for small K), the fate of these non-resonant and resonant tori are given by the KAM theorem and Poincaré-Birkhoff theorem. The irrational tori survives under small perturbations due to the KAM theorem, as we can see in fig.2.3 (a) and (b). As we increase K further, these tori also start breaking, and the last irrational tori breaks⁷ at $K \approx 0.971635$. The last irrational tori correspond to the case when p_0 is the golden ratio, $\frac{\sqrt{5}-1}{2}$, which is the most irrational number. So, the irrational tori,

⁷This value is determined by renormalization group technique [13]-[14].

in some sense, breaks depending on their degree of irrationality as we vary K .

- **Spread of Chaos:**

For small K (less than 1), the chaos is restricted between the irrational tori as illustrated in Fig. 2.3. The trajectories lying in between two irrational tori do not cross. Thus, the presence of these irrational tori prevents the widespread of the trajectories in the phase space. But, once the irrational tori starts breaking, the trajectories are no longer confined between these irrational curves, and the curve wanders all over the phase space. This leads to chaos as we increase K further. We go from regularity to completely chaotic with intermediate phase space being mixed, fig. 2.3.

2.5 Coupled Standard Map:

We can have two standard maps coupled together to get a 4D map. It was first studied in ref. [15]. The Hamiltonian, H for the coupled standard map is then given as -

$$H(q_1, q_2, p_1, p_2) = H_1(q_1, p_1) + H_2(q_2, p_2) + H_b(b, q_1, q_2) \quad (2.15)$$

where, $H_1(q_1, p_1)$, $H_2(q_2, p_2)$ and $H_b(b, q_1, q_2)$ are given as -

$$H_1 = \frac{p_1^2}{2} - \frac{K \cos(2\pi q_1)}{(2\pi)^2} \sum_{n=-\infty}^{\infty} \delta(t/T - n) \quad (2.16.a)$$

$$H_2 = \frac{p_2^2}{2} - \frac{K \cos(2\pi q_2)}{(2\pi)^2} \sum_{n=-\infty}^{\infty} \delta(t/T - n) \quad (2.16.b)$$

$$H_b = \frac{b}{(2\pi)^2} \cos(2\pi(q_1 + q_2)) \quad (2.16.c)$$

where b is the coupling/interaction strength between the two standard maps. The map corresponding to the Hamiltonian, H , is then given as-

$$q'_1 = q_1 + p_1 \quad (2.17.a)$$

$$p'_1 = p_1 - \frac{K}{2\pi} \sin(2\pi q'_1) + \frac{b}{2\pi} \sin(2\pi(q'_1 + q'_2)) \quad (2.17.b)$$

$$q'_2 = q_2 + p_2 \quad (2.17.c)$$

$$p'_2 = p_2 - \frac{K}{2\pi} \sin(2\pi q'_2) + \frac{b}{2\pi} \sin(2\pi(q'_1 + q'_2)) \quad (2.17.d)$$

The map is connecting states just after two consecutive kicks. The phase space is now a 4D torus, and we have mod one operation in all four equations. For $b = 0$, we have two uncoupled standard maps. Analysing the phase space for this map is not easy as it is 4D. We shall be using this to study the relationship between entanglement and chaos. As well as use it in unitary circuits and study the resulting channel.

In this chapter, we have gotten some understanding of the classical behaviour of a single standard map which shows a transition to chaos as we vary the parameter. As we vary K slightly, the rational tori breaks, but the irrational tori survives and then starts to break depending on the extent of their irrationality. The last of them break at around $K = 0.97$. The presence of irrational tori prevents the widespread of chaos, but for $K > 1$, trajectories start to wander over the entire phase space. The phase space of a standard map shows rich behaviour, which makes it more interesting, and that is why it is still being studied by physicists. We would like to examine the quantum effects of these underlying rich classical dynamics by quantizing the standard map.

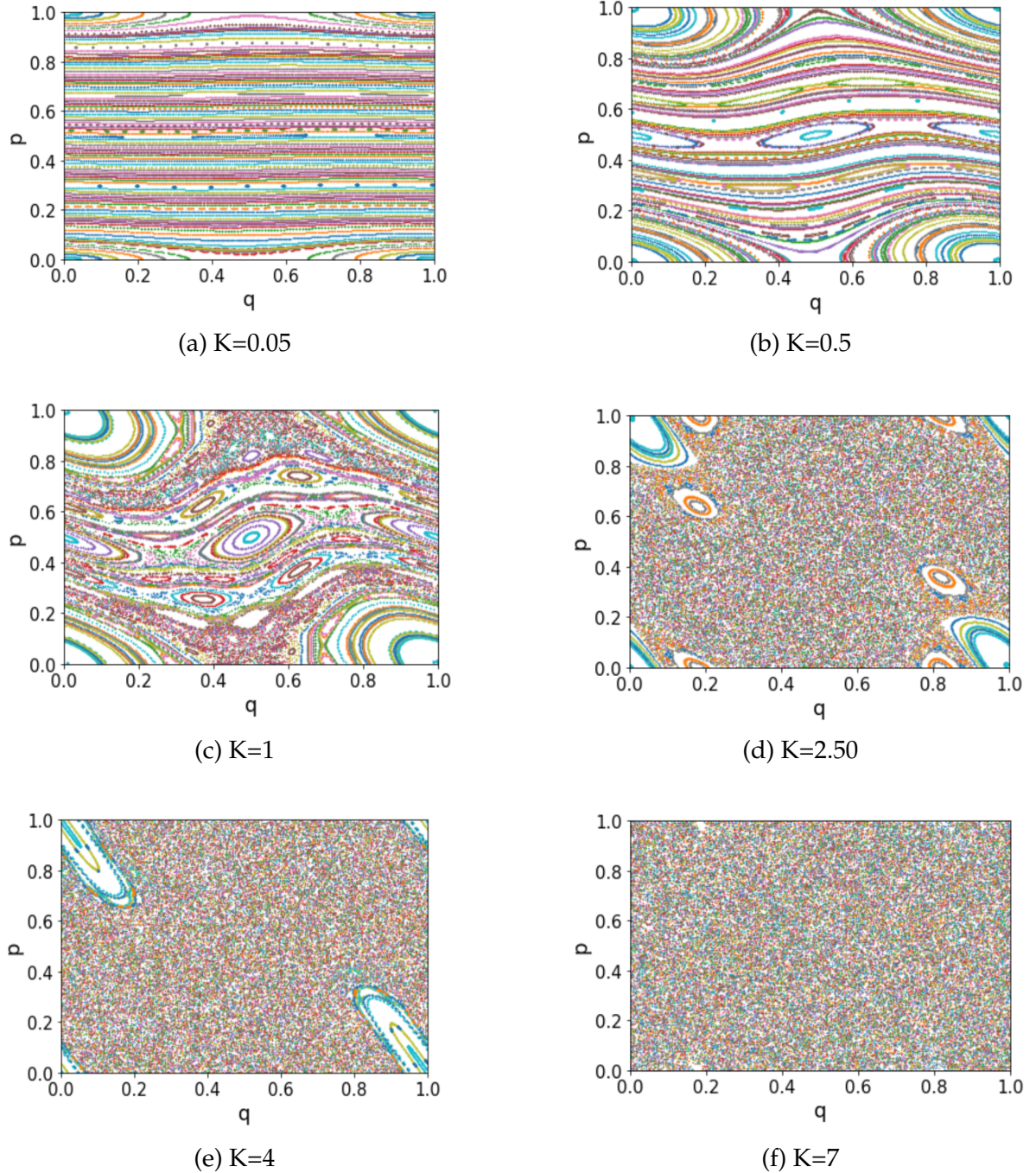


Figure 2.3: The phase space plot for the standard map for 300 initial points iterated over 700-time steps. The q and p both vary from 0 to 1.

Chapter 3

Preliminaries

Before going into Quantum chaos, let us look at some of the basic concepts which will be used later.

3.1 Entanglement

Entanglement is an interesting phenomenon that occurs in a composite quantum system. Suppose we have a composite quantum system of two parties(bipartite), A and B. If \mathcal{H}_A and \mathcal{H}_B are the Hilbert spaces of A and B respectively, then $\mathcal{H} = \mathcal{H}_A \otimes \mathcal{H}_B$ will be the Hilbert space of the bipartite system, AB. Now, if $|\psi\rangle$ is a bipartite pure state and $|\psi_A\rangle$ is the state of subsystem A alone, and $|\psi_B\rangle$ is the state of B alone then, for A and B to be entangled we cannot write - $|\psi\rangle = |\psi_A\rangle \otimes |\psi_B\rangle$. Thus, an entangled state is one which cannot be written in a product form. An example of an entangled state is -

$$|\psi\rangle = \frac{1}{\sqrt{2}} (|00\rangle + |11\rangle) \quad (3.1)$$

One can easily verify that we cannot express this in product form. In fact, it is a maximally entangled state and is one of the four Bell states. It is maximally entangled because a measure of entanglement (which we define later) saturates to the maximum value for this state. The maximally entangled state is defined as -

$$|\phi_{AB}\rangle = \frac{1}{d} \sum_{i=1}^d |i_A\rangle |i_B\rangle \quad (3.2)$$

where, d = local dimension of the H_A and H_B and $\{i_A\}$ and $\{i_B\}$ are the orthonormal basis for the two subsystem.

We should note that Entanglement is different from classical correlation. Suppose we have classically correlated pairs $|00\rangle$ and $|11\rangle$ mixed with probabilities $1/2$. In this case, the state in eq. 3.1 and the classical result will match for Z measurement, but now if we do other measurements on classical pairs, we would not be able to see such correlations. On the other hand, for an entangled state, the correlation is still there in another basis. Thus, entanglement is independent of the choice of measurement we make, which makes it interesting and differentiates it from classical correlations.

3.2 Density Matrix and Reduced Density Matrix

- **Density Matrix:**

The state of the system for a composite quantum system may not always be pure, and in general, we have mixed states. This gives rise to the concept of density operator or density matrix in quantum mechanics.

If we have a collection of pure quantum states, $\{|\psi_i\rangle\}$ occurring with classical probabilities, $\{p_i\}$ and $\sum_i p_i = 1$, then the density matrix for the ensemble $\{p_i, |\psi_i\rangle\}$ is defined as -

$$\rho = \sum_i p_i |\psi_i\rangle\langle\psi_i| \quad (3.3)$$

Here, ρ is a mixed state but for a pure state, $|\psi\rangle$, ρ is given as -

$$\rho = |\psi\rangle\langle\psi| \quad (3.4)$$

Properties of Density Matrix:

- $\text{Tr}(\rho) = 1$. This is due to the fact that $\sum_i p_i = 1$.
- $\rho \geq 0$. ρ is a positive operator. A is a positive operator if $\langle\phi|A|\phi\rangle \geq 0 \forall |\phi\rangle$. Positive operators are Hermitian but not vice-versa.
- For pure state, $\rho^2 = \rho$ and $\text{Tr}(\rho^2) = 1$ and for mixed states, $\text{Tr}(\rho^2) \leq 1$.

We can now use the density matrix to describe the state of the system. This is because we can define the evolution of the system, measurements and expectations values in terms of the density matrix [16].

- **Reduced Density Matrix**

In a composite system, there are instances where we wish to just look at the subsystems. This is attained by the concept of a reduced density matrix which allows us to describe the individual subsystems in a composite system. For a bipartite system, AB, the reduced density operator of subsystem A is defined as -

$$\rho_A = \text{tr}_B(\rho_{AB}) \quad (3.5)$$

where, ρ_{AB} is the density operator for the bipartite system, AB and tr_B is the partial trace [16]. Similarly, we can define the reduced density operator for B as -

$$\rho_B = \text{tr}_A(\rho_{AB}) \quad (3.6)$$

3.3 Schmidt Decomposition

Schmidt Decomposition is a powerful tool in quantum information theory. It applies only to the case of bipartite systems. If for a pure bipartite quantum state with the dimension of the subsystems as d , we can write this state as the sum of d orthonormal product states, then such a decomposition is known as Schmidt Decomposition.

Suppose $|\psi_{AB}\rangle$ is a pure bipartite state; then we can write this state as -

$$|\psi_{AB}\rangle = \sum_{i,j=1}^d c_{ij} |ij\rangle_{AB} \quad (3.7)$$

where, $\{|i_A\rangle\}$ and $\{|j_B\rangle\}$ is the orthonormal basis with dim, d for the subsystem A and B respectively and $|ij\rangle_{AB}$ are the tensor product of the two bases and it is the orthonormal basis for the system, AB with dim, d^2 . By Schmidt decomposition, we can write the same state as -

$$|\psi_{AB}\rangle = \sum_{k=1}^d \sqrt{\lambda_k} |k_A\rangle |k_B\rangle \quad (3.8)$$

Here, $|k_A\rangle$ and $|k_B\rangle$ are known as Schmidt bases for A and B and are unique up to local unitary transformations. $\{\lambda_k\}$ are non-negative real numbers that sum up to 1, and they are known as Schmidt value. $\{\lambda_k\}$ are the eigenvalues of the reduced density matrix ρ_A or ρ_B and are invariant under local unitary transformations.

Thus, we have written the state, $|\psi_{AB}\rangle$ as the linear combination of d orthonormal product states of composite system AB. Going from eq. 3.7 to eq. 3.8 involves local unitary rotations in subsystems A and B. The complete proof of this is given in Appendix A.

For unentangled states, we have only one non-zero Schmidt value, which is one because, in that case, we can express $|\psi_{AB}\rangle$ as a product state. We can also write Schmidt decomposition for a bipartite system with the dimensions of subsystems being different. In this case, it is given as-

$$|\psi_{AB}\rangle = \sum_{k=1}^{\min(d_A, d_B)} \sqrt{\lambda_k} |k_A\rangle |k_B\rangle \quad (3.9)$$

The Schmidt decomposition is useful in many areas of quantum information, including quantum entanglement theory, quantum communication, and quantum computation. It provides a powerful tool for understanding the structure of entanglement in bipartite quantum systems.

3.4 Von Neumann Entropy

The von Neumann Entropy is defined as -

$$S(\rho) = - \text{tr}(\rho \log(\rho)) \quad (3.10)$$

The log is taken in base 2. In terms of eigenvalues of ρ we get-

$$S(\rho) = - \sum_{i=1}^d \lambda_i \log(\lambda_i) \quad (3.11)$$

where ρ is a $d \times d$ matrix and we know, $\sum_{i=1}^d \lambda_i = 1$.

The maximum value of $S(\rho)$, when all λ_i 's are equal, is $\log d$ which is for maximally mixed states, and it is 0 for pure states. Hence, it measures the degree of "mixedness" of a quan-

tum state. von Neumann entropy is also used to quantify the amount of entanglement in a composite quantum system. For a bipartite system, the entanglement entropy, a measure of entanglement, is then given by the von Neumann entropy of the reduced density operator of one of the subsystems.

$$S = -\text{tr}_A(\rho_A \log(\rho_A)) = -\text{tr}_B(\rho_B \log(\rho_B)) \quad (3.12)$$

The above equation holds for pure state only. For mixed states, in general, $S(\rho_A) \neq S(\rho_B)$.

There are various other measures of entanglement like, Renyi entropy, and linear entropy[16].

Chapter 4

Quantum Chaology

With the advent of Quantum Mechanics, physicists realized that classical mechanics is incomplete. Classical mechanics arise as a limit of quantum mechanics, and there are certain interesting quantum phenomena with no classical analogue. Since classical mechanics arises as a limit of quantum mechanics, we would not be surprised to see some chaotic behaviour in quantum mechanics. The state of the system in quantum mechanics is given by wave function, which follows Schrodinger's equation. We have seen in classical mechanics that chaos arises for non-linear systems. But, since Schrodinger's equation is linear, we cannot get sensitive dependence on initial conditions which is a key feature of classical chaos.

Also, due to Heisenberg's uncertainty principle, the notion of trajectories is missing from the quantum regime. So, there cannot be any exponential divergence of trajectories, which again is a key feature of classical chaos. So, there is no theory of Chaos that is defined for a Quantum state.

4.1 What is Quantum Chaos?

Many scientists have observed many unique behaviours in the quantized version of classical systems, which are chaotic, such as spectral level repulsion, dynamical localizations in time evolution, etc. But, a general theory of quantum chaos was still lacking. As semiclassical theory[17] developed, the answer to what quantum chaos is, was addressed by many physi-

cists but mainly by, M Gutzwiller and M V Berry. A definition of quantum chaos as given by Berry[18] is -

"Quantum Chaology¹ is the study of semiclassical, but non-classical, behaviour characteristic of systems whose classical dynamics exhibits chaos."

So, in this field, we try to answer questions like what is the effect of classical chaos on the quantum system in the semi-classical regime. We will see that in the quantized version of classical systems, we get interesting signatures of chaos in the quantum regime when the classical system is in the chaotic region, which is different from the regular region of the underlying classical system. The study of Quantum Chaos has applications in condensed-matter physics, many cold-atom experiments and many-body systems. It is still a developing area, and many questions are yet to be answered, which makes it more interesting.

4.2 Quantum Maps

Quantization of classical maps gives Quantum Maps. The field of quantized chaotic systems began with quantizing one dof non-autonomous systems(1.5 dof systems), mainly of kicked type and some maps like cat map[19] and baker's map. The starting works were done by two groups, one was by G. Casati, B. V. Chirikov, F. M. Izraelev, and J. Ford [20] and another was by N . L . Balazs, A. Voros, M . V . Berry and M. Tabor in ref [21]-[22]. Quantum maps have been realized experimentally, and interesting phenomena like dynamical localization have been observed.

Classical maps are given by canonical transformations and the quantum equivalent of which is a unitary operator. Getting this equivalence is simpler for Kicked Hamiltonian Systems, described in Chapter 1. From sec 2.4, we have the form of Kicked Hamiltonian Systems as -

$$H = f(p) + V(q) \sum_{n=-\infty}^{\infty} \delta(t/T - n) \quad (4.1)$$

In the classical case, we have the stroboscopic map, which relates the phase space variables immediately after the n^{th} and $(n + 1)^{th}$ kick. If we can find a unitary operator which re-

¹Berry referred to it as Quantum Chaology instead of Quantum Chaos.

lates the state of the system after n^{th} and $(n + 1)^{th}$ kick, then that unitary will represent the Quantum Map. It can be written as -

$$|\psi_{n+1}\rangle = U|\psi_n\rangle \quad (4.2)$$

here, $|\psi_n\rangle$ = state just after n^{th} kick. On solving Schrödinger's Equation for the Hamiltonian in eq.4.1 we get -

$$|\psi_{n+1}\rangle = \exp(-iVT/\hbar) \exp(-ifT/\hbar)|\psi_n\rangle \quad (4.3)$$

It is solved in appendix B. Therefore,

$$U = \exp\left(\frac{-iV(q)T}{\hbar}\right) \exp\left(\frac{-if(p)T}{\hbar}\right) \quad (4.4)$$

Thus, we have got the quantization of classical maps for a class of Kicked Hamiltonian System. We will focus on Standard Map or Kicked Rotor.

4.2.1 Quantum Standard Map

Quantum Standard Map or Quantum Kicked Rotor is obtained by quantizing Classical Standard Map. It was first studied by G. Casati, B. V. Chirikov, F. M. Izraelev and J. Ford in ref [20], and experimental realizations were achieved by the Mark G. Raizen group in 1995 and later by the Auckland group.

The quantization of classical standard map yields -

$$U = \exp\left(\frac{igT}{(2\pi)^2\hbar} \cos(2\pi q)\right) \exp\left(\frac{-iT}{2\hbar} p^2\right) \quad (4.5)$$

Note that, U can be expressed as a product of two unitaries. Quantization can either be on a cylinder or a torus, as illustrated in ref [7]. In the case of a cylinder, U is an infinite-dimensional matrix, whereas, it is a finite-dimensional matrix on a torus. So, in order to avoid infinity, we do the quantization on the torus, which will give a finite-dimensional unitary matrix, U .

4.2.2 Quantization on Torus

On torus, both q and p are restricted between 0 and 1 for the classical map. The momentum and position eigenbasis is infinite-dimensional but when we impose the condition restricting the dynamic on a torus, we get a finite-dimensional state space both in position and momentum[7]. Let the position and momentum basis be $\{q_n\}$ and $\{p_n\}$ and $\{n=0,1,2,\dots,N-1\}$. Here, N is the dimension of the Hilbert space and $N=1/\hbar$.

The position and momentum translation operator are respectively given as -

$$T_q = \exp\left(\frac{-ip\Delta q}{\hbar}\right) \quad (4.6.a)$$

$$T_p = \exp\left(\frac{iq\Delta p}{\hbar}\right) \quad (4.6.b)$$

Since we have a finite number of basis elements. The action of the above operators on momentum and position basis sets is given as -

$$\langle q_n | T_q = \langle q_{n+1} |; \quad \langle q_n | T_q^N = \exp(2\pi i \beta) \langle q_n | \quad (4.7.a)$$

$$T_p | p_n \rangle = | p_{n+1} \rangle; \quad T_p^N | p_n \rangle = \exp(2\pi i \alpha) | p_n \rangle \quad (4.7.b)$$

Here, α controls parity symmetry and β controls time-reversal symmetry and is the phase accumulated as we move along q direction. α and β lie in the range $[0,1)$. α and β is zero for periodic boundary condition and $1/2$ for anti-periodic conditions.

We have shown in appendix B that the below equations hold.

$$T_q | p_m \rangle = \exp\left(\frac{2\pi i}{N}(m + \beta)\right) | p_m \rangle \quad (4.8.a)$$

$$T_p | q_n \rangle = \exp\left(\frac{2\pi i}{N}(n + \alpha)\right) | q_n \rangle; \quad (4.8.b)$$

$$\langle q_n | p_m \rangle = \frac{1}{\sqrt{N}} \exp\left(\frac{2\pi i}{N}(n + \alpha)(m + \beta)\right) \quad (4.9)$$

Thus, from eq. 4.8, we can conclude that the eigenvalues of position and momentum opera-

tors are -

$$q_n = \frac{n + \alpha}{N} \quad (4.10.a)$$

$$p_n = \frac{m + \beta}{N} \quad (4.10.b)$$

4.2.3 Coherent States on the Torus

Coherent states are a class of quantum states introduced by physicist Erwin Schrödinger in the 1920s. They are called coherent because they exhibit a classical-like behaviour in certain respects, such as having a well-defined position and momentum. Coherent states are minimum uncertainty states and are also "localized" in phase space. They are significant in studying quantum systems that exhibit semiclassical behaviour, where quantum mechanics and classical mechanics overlap.

Schrödinger introduced it in the case of the harmonic oscillator as the eigenstates of the annihilation operator. Coherent states on the torus are equivalent to that of a harmonic oscillator. In the case of the harmonic oscillator, the ground state was a coherent state which is then acted upon by a displacement operator to generate the entire coherent state basis. For the case of coherent states on the torus, it was proposed by M.Saraceno in ref [23], to start with the state, which is the ground of the Hamiltonian -

$$H = 2 - \frac{1}{2} (T_q + T_q^\dagger + T_p + T_p^\dagger) \quad (4.11)$$

The ground state which one obtained is localized as $q = 0$ and $p = 0$ as we can see in Fig. 4.6(a).

Let us call this state $|00\rangle$. The coherent state basis is then obtained by translating this state in the phase space using translation operators, appendix B. Thus, a coherent state localized at a certain value of p and q is then given by[as shown in Fig. 4.6 b), c) and d)]

$$|pq\rangle = T_p^p T_q^q |00\rangle ; \quad 0 \leq p, q \leq N - 1 \quad (4.12)$$

The coherent state generated can then be used to get a phase space representation of a quantum state, $|\psi\rangle$. The overlap of any quantum state given as -

$$H(p, q) = |\langle pq|\psi\rangle|^2 \quad (4.13)$$

where, $H(p, q)$ is known as Husimi or coherent state representation and in a way, it tells us about the spread of a quantum state in position and momentum.

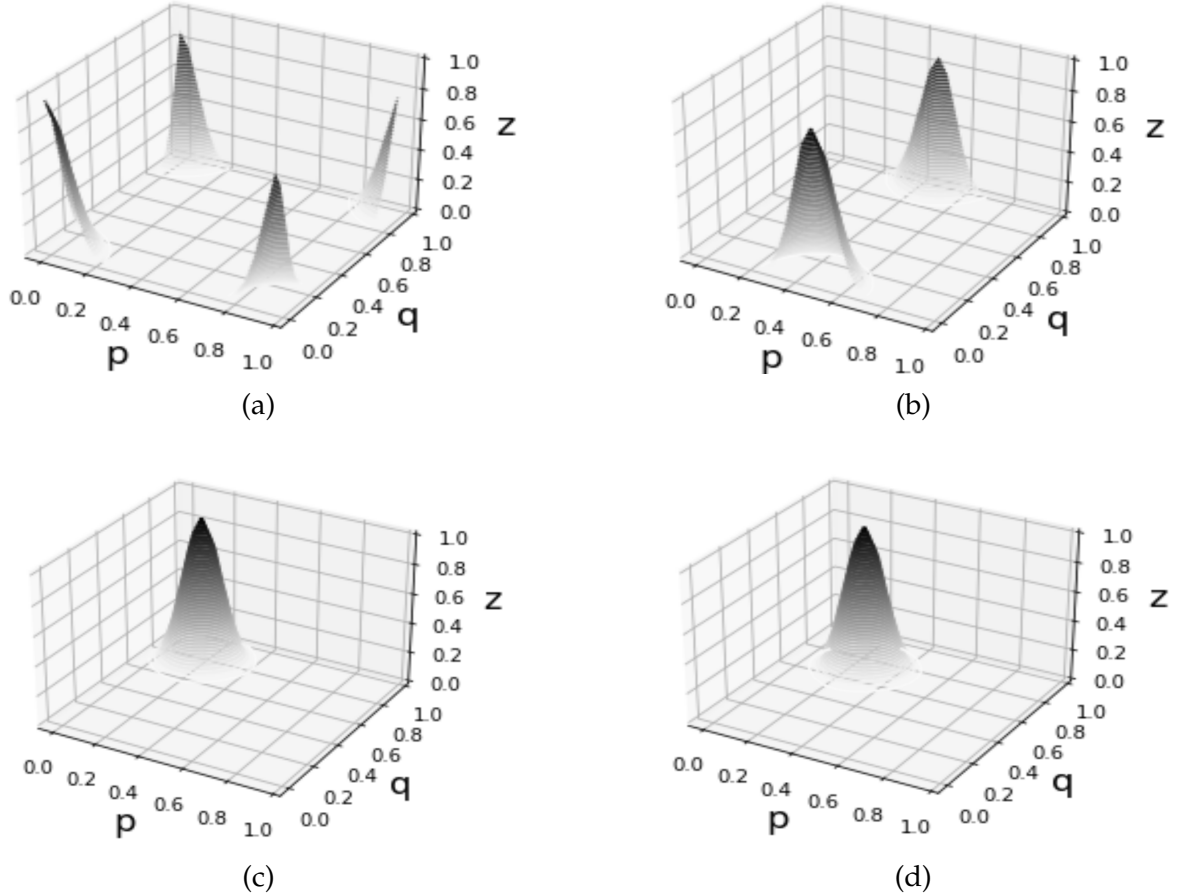


Figure 4.1: 3D plots representing the matrix elements of Coherent States at- a) $p=q=0$, b) $p=0.479$ and $q=0$, c) $p=0.2$ and $q=0.76$, d) $p=0.28$ and $q=0.68$. Here, the z-axis represents the magnitude of the state at particular p and q .

4.2.4 Quantum Map on Torus

We can write our Unitary, U obtained by quantization of map in sec.4.2.1 in either position or momentum basis obtained in case of a torus. We chose to represent it in a position basis. From eq. 4.4 we have-

$$U = \exp\left(\frac{-iV(q)T}{\hbar}\right) \exp\left(\frac{-if(p)T}{\hbar}\right) \quad (4.14)$$

For the map to be restricted on a unit torus, $f(p)$ and $V(q)$ both should be periodic functions of the unit period. Hence, the matrix representation of U in position basis is given as -

$$U_{nn'} = \langle q_n | \exp\left(\frac{-iV(q)T}{\hbar}\right) \exp\left(\frac{-if(p)T}{\hbar}\right) | q_{n'} \rangle \quad (4.15)$$

On using eq. 4.9 and 4.10, we get² -

$$U(n, n', \alpha, \beta, K) = \frac{1}{N} \exp\left(-2\pi i NV\left(\frac{n' + \alpha}{N}\right)\right) \sum_{m=0}^{N-1} \exp\left(-2\pi i Nf\left(\frac{m + \beta}{N}\right)\right) \exp\left(\frac{2\pi i}{N}(m + \beta)(n - n')\right) \quad (4.16)$$

This is the matrix form of U , which is the quantization of a kicked Hamiltonian system on a torus.

4.2.5 Representing Quantum Standard Map on Torus

We have stated that for quantization on a torus, $V(q)$ and $f(p)$ should be periodic functions. We choose the time period to be 1. Thus, $T = 1$ and $K = g$ as $K = Tg$. Therefore, the unitary, U from eq. 4.5 can be re-written as-

$$U = \exp\left(\frac{iK}{(2\pi)^2 \hbar} \cos(2\pi q)\right) \exp\left(\frac{-i}{2\hbar} p^2\right) \quad (4.17)$$

Therefore, using eq. 4.16 we can write the matrix form of U for a standard map as -

$$U(n, n', \alpha, \beta, K) = \frac{1}{N} e^{\left(\frac{iNK}{2\pi} \cos(2\pi \frac{n' + \alpha}{N})\right)} \sum_{m=0}^{N-1} e^{\left(-\pi i \left(\frac{(m + \beta)^2}{N}\right)\right)} e^{\left(\frac{2\pi i}{N}(m + \beta)(n - n')\right)} \quad (4.18)$$

4.2.6 Coupled Quantum Standard Map

Just like in classical mechanics, we discussed coupled standard maps with phase space being a 4D torus. We can do a similar coupling for the quantum standard maps, which will be the quantization of coupled classical standard map on a 4D torus. The motivation behind coupling two systems is to find the relation between Entanglement and Chaos, as we shall see. The unitary, in this case, is given as -

$$U = (U_1 \otimes U_2)U_b \quad (4.19)$$

²The exact derivation is done in Appendix B

Here, U_1 is the quantization of the first standard map with parameter K_1 and, U_2 is the quantization of the second standard map with parameter K_2 and U_b is the quantization corresponding to the interaction we had in the classical case.

$$U_1 = U(n_1, n'_1, \alpha, \beta, K_1) \quad (4.20.a)$$

$$U_2 = U(n_2, n'_2, \alpha, \beta, K_2) \quad (4.20.b)$$

$$U_b = \exp \left(\frac{-iNb}{2\pi} \cos \left(\frac{2\pi}{N}(n_1 + n_2 + 2\alpha) \right) \right) \delta_{n_1, n'_1} \delta_{n_2, n'_2} \quad (4.20.c)$$

U_1 and U_2 is determined by eq 4.18 . Note that U_b is a diagonal matrix.

4.3 Relation Between Entanglement and Chaos

" Uniting The Two Mysteries! "

Due to being a non-local behaviour, entanglement was considered a paradox. But as we are moving to the era of quantum computers, entanglement has been a handy resource. Entanglement is one of the critical reasons for the supremacy of quantum algorithms.

There have been studies to find the effects of classical chaos on quantized systems, and indeed, there have been many quantum signatures of chaos on energy level separation, localization, etc. So, it will be interesting to see the effect of chaos on the other. Basically, **How does Chaos affect the Entanglement?** Quantum computers are many-body interacting systems. Thus, chaos is unavoidable and also, due to interaction, the bodies might get entangled. We can have some signatures of chaos or quantum chaos. Hence, it is essential to try to connect the two concepts.

Also, entanglement can be created by unitary operators or arises due to symmetry. We have seen that unitary operators can be obtained by exponentiation of the system's Hamiltonian. If we choose a classical Hamiltonian that can show chaotic behaviour as we vary the control parameter. It is natural to ask what's the difference between entanglement produced when it is either integrable or chaotic. As we shall see, there is quite some difference between regular and chaotic cases.

The first work in this regard was done in 1998[24] with the motivation to establish entanglement as an indicator of chaos. There have been plenty of works after that by scientists in the field of condensed matter, statistical and quantum information, and it is still growing. It is also gaining more popularity as the world is heading towards quantum computers to explore whether chaos suits Quantum Supremacy.

In the work by A.Lakshminarayan in Ref [25], the relation between entanglement and chaos has been explored for Coupled Standard Map. The author has used a Coupled Standard Map, to study the relation and has shown quantum signatures of classical chaos. For a basic understanding of this relation, we have focused on this work and tried to reproduce some of the results in the paper. Hence, the following section is a detailed summary of this work.

4.4 Numerical Results

Coupled Quantum Standard Map can be considered a bipartite system. If \mathcal{H} be the state space of the bipartite system then, $\mathcal{H} = \mathcal{H}_1 \otimes \mathcal{H}_2$ and dim of $\mathcal{H} = N^2$ where, $N = \text{dim of } \mathcal{H}_i$ and $\{i=1,2\}$. Let us take a pure state, $|\psi\rangle \in \mathcal{H}$. We then have reduced density matrices for subsystems 1 and 2 as ρ_1 and ρ_2 . We have seen a measure of entanglement in Chapter 1. We will use von-Neumann entropy as the measure in our study³. Sometimes, we will refer to this as entanglement or simply as entropy.

4.4.1 Entanglement Entropy

Entanglement entropy is given as⁴ -

$$S(\rho) = -\text{tr}_1(\rho_1 \log(\rho_1)) = -\text{tr}_2(\rho_2 \log(\rho_2)) \quad (4.21)$$

In the Schmidt basis⁵,

$$|\psi\rangle = \sum_{i=1}^N \lambda_i |\phi_i^{(1)}\rangle |\phi_i^{(2)}\rangle \quad (4.22)$$

³This is because it is local unitary invariant.

⁴It doesn't matter whether we take ρ_1 or ρ_2 as we had a pure state. For mixed states, this is not true in general

⁵defined earlier in chapter 3

$\{\lambda_i\}$ are the eigenvalues of ρ_1 and ρ_2 . We can then express eq 4.21 in terms of these λ'_i s as-

$$S(\rho) = - \sum_{i=1}^N \lambda_i \log(\lambda_i) \quad (4.23)$$

For a coupled standard map, the unitary U is given as in eq.4.19. If we take the initial state to be unentangled, then after the action of U , the states will get entangled except when $b=0$. Thus, we can argue that the entangling property of the system is due to the inherent entanglement in the eigenstates of the operator, U . Let- $|\psi_i\rangle$, $\{i=1,2,\dots,N^2\}$ represent the stationary states or the eigenstates of U .

- **Average Entanglement Entropy:**

We define average entropy with an average over the entire spectrum, and it is given as

$$\bar{S} = -\frac{1}{N^2} \sum_{i=1}^{N^2} \text{tr}_1 (\rho_{1i} \log(\rho_{1i})) \quad (4.24)$$

where $\rho_{1i} = |\psi_i\rangle\langle\psi_i|$. We first calculate the eigenstates of U for the case when $K_1 = 0.1$, $K_2 = 0.15$, $\alpha=0.35$ and $\beta=0$. α and β control the parity and time symmetry in the system. We do not want to break the time symmetry, and thus, we choose $\beta = 0$. However, if we have parity symmetry, we would have to bother about degeneracies in the eigenstates and for that reason, we chose $\alpha = 0.35$ so that there is no parity symmetry. This is because one just wants to study the entanglement properties of the eigenstate. The value of K_1 and K_2 is chosen such that there is no chaos in the uncoupled case. This will help us better understand the relationship between chaos due to interaction and entanglement produced by it. We plot \bar{S} as a function of b , and the result is given in Fig. 4.2.

From the graph, we see that \bar{S} grows linearly with b , and after a particular value of b (≈ 2), \bar{S} saturates to a specific value which depends on the dimension of the subsystem.

We can thus say that chaos is assisting entanglement between the two subsystems. The flattening of the curve might represent uniform classical chaos in the system. Hence, \bar{S} can show the transition which leads to chaos. This transition is not easy to see classically, as we have 4D phase space, which is challenging to analyze. Here we can see that

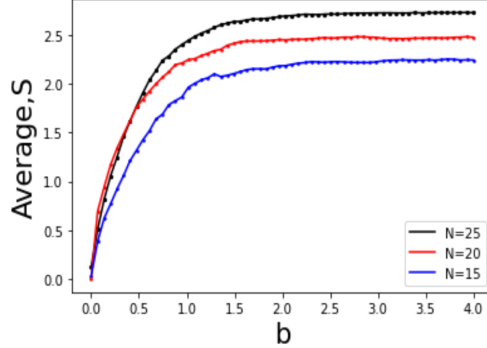


Figure 4.2: \bar{S} vs b for $K_1 = 0.1, K_2 = 0.15$

entanglement depends on the system's dynamics and can also indicate the transition to chaos.

For a maximally entangled state, the entropy is maximum, and its value is $\log(N)$, where N is the dimension of the subsystem. Our curve shows that the saturation value is $\log(N) - 0.5$. This is precisely the value that we get from random matrix theory⁶(RMT)[26]-[27]. This confirms that our system is chaotic when \bar{S} saturates.

- **Entropy of Individual States:**

Now, to know more about the entanglement and chaos, we see the plot of entropy for the individual stationary states for the case when $b=2$, i.e., the underlying system is chaotic. The value of other parameters is the same as in the previous figure 4.2. The required plot is represented in Fig 4.3.

From the figure, it is evident that for most of the states, entropy is near $\log(N) - 0.5$, which is the saturation value, but there are a few whose entropy is remarkably less than this value. Such low entropy states are expected to be localized in phase space.

4.4.2 Eigenstates and Reduced Density Matrix

- **Eigenstates or Stationary States of U:**

⁶From RMT, we have that if the underlying system is chaotic and we have a unitary, U corresponding to quantized maps, then we can mimic the same results obtained by U by using a random unitary from an ensemble. The choice of the ensemble is a different story.

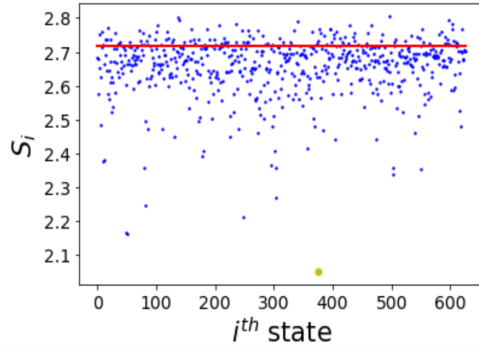


Figure 4.3: Entropy, S of eigenstate, $|\psi_i\rangle$ for $K_1 = 0.1$, $K_2 = 0.15$, $N = 25$ and $b = 2$. The red line is corresponding to the saturation value $\log(N) - 0.5$ of the average entanglement entropy

From Fig. 4.3, it is evident that there are two classes of eigenstates. One for which the entropy is near the saturated value and the other whose entropy is less than this value. We call the first class of eigenstates, delocalized states and the latter, localized states. The choice of name will be evident as we plot the eigenstate corresponding to these states. We now chose a delocalized state with entropy as $\log(N) - 0.5$ and a localized state as the state with the least entropy (marked with a yellow dot in fig. 4.3) from the entire spectrum and Fig. 4.4 gives the 2D plot for the two states. For a delocalized state,

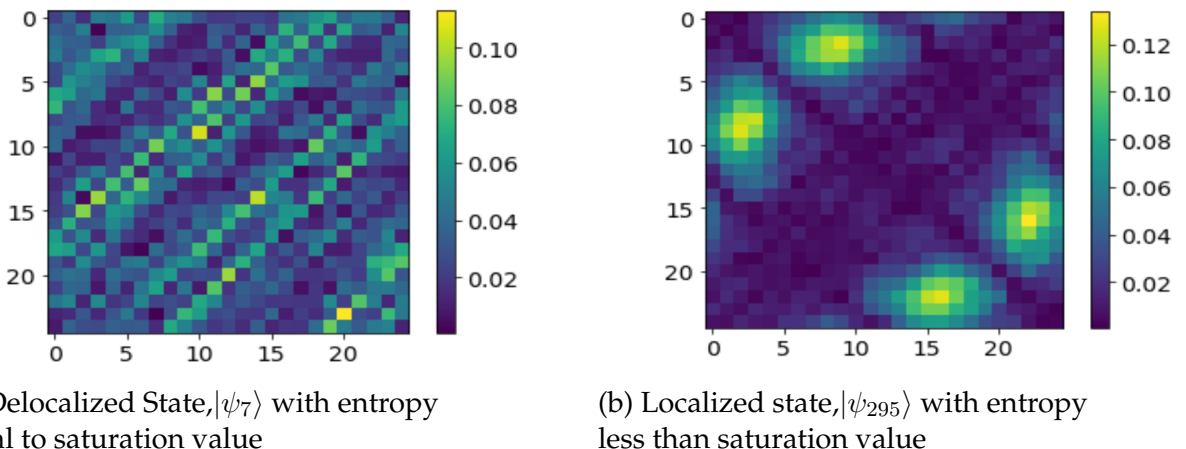
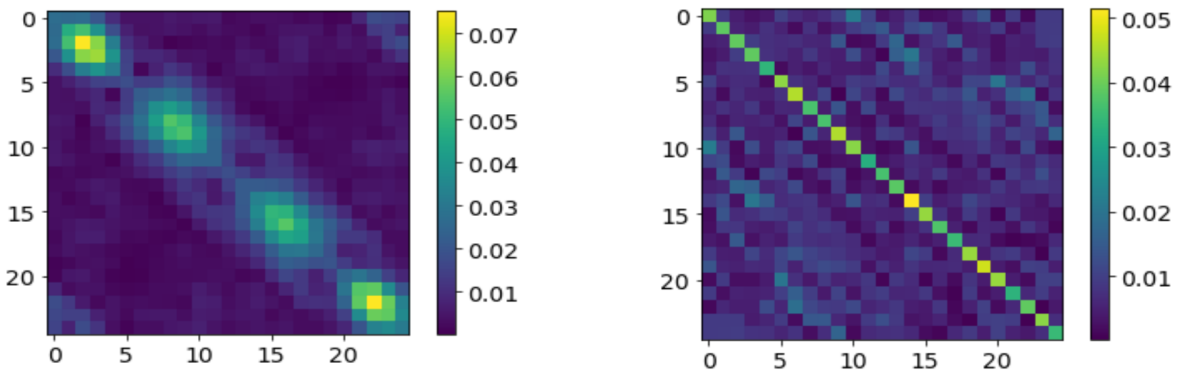


Figure 4.4: A 2D plot of - a) Delocalized state and b) Localized state. The colorbar corresponds to the magnitude of the eigenstate. X and Y are nothing but indices of the eigenstate matrix. The plot represents the absolute value of the matrix elements of the corresponding state.

the state is spread. Hence, the name is delocalized. On the other hand, a low entropic state is highly localized. Many states in the localized class have the same structure and thus represent some "scarring" of states. Scarring was first presented by Eric Heller in [1]. He showed that many of the eigenfunctions for the chaotic stadium billiard were having close resemblance with classical periodic orbits, and he referred to these as "scars" of a periodic orbit in the quantum eigenfunctions. Hence, entanglement is highly dependent on the localization of states or scarring. And is less for localized states when compared with a delocalized state.

- **Reduced Density Matrix, (RDM):**

Next, we can plot the reduced density matrix for the subsystems corresponding to the localized and delocalized state. Since entanglement is nearly maximal for a delocalized state, we expect it to be diagonally dominant. But, we observe that the reduced density matrix for a localized state is more cleanly diagonal.



(a) Reduced density matrix, $|\rho_7^{(1)}\rangle$ of subsystem,1 corresponding to delocalized eigenstate, (b) Reduced density matrix, $|\rho_{205}^{(1)}\rangle$ of subsystem,1 corresponding to localized eigenstate,

Figure 4.5: A 2D plot of RDM of subsystem 1, for a) Delocalized state and b) Localized state. The RDM is more cleanly diagonal in b).

- **Eigenvalues of Reduced Density Matrix:**

Given a reduced density matrix, what more can we say about the states? If we look at the spectra of the two reduced density matrices, we will observe that the information about the localization is stored in eigenvalues in a graded way[25]. We arrange the eigenvalues in increasing order and then plot them for a localized and a delocalized

state. Fig 4.6 represents this, and we can see that the first few eigenvalues behave differently for the localised state. After some initial values, the trend is the same for the case of localized and delocalized cases.

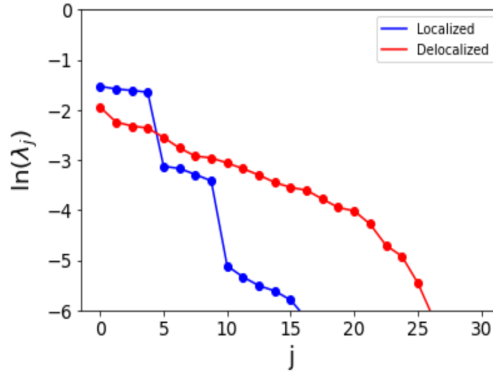


Figure 4.6: Log of eigenvalues of RDM of the subsystem,1 for localized and delocalized states. The first few eigenvalues of a localized state have some near degeneracy which is not present for a delocalized state.

An interesting thing to note is that for localized cases, there are levels of near-degenerate eigenvalues with degeneracy 4. The near degeneracies of the eigenvalues have been explored in Ref [28].

In this chapter, we have clearly seen the quite different quantum effects corresponding to the underlying classical dynamics. We have closely seen the effect of chaos in the entanglement in Fig. 4.2 and also how entanglement entropy can be used to see a transition from regularity to chaos to some extent. The scarring of quantum states by classical periodic orbits was also observed, and we illustrated that the information about this localization is also stored in the Schmidt coefficients in a graded manner. The husimi of the Schmidt vectors gives better insight into the corresponding classical periodic orbit that scars the quantum eigenstates. In ref [25], the scarring by a classical periodic orbit for the coupled standard map was presented.

Having said all that, we would move to the central part of this work with quantum channels. So far, the system we were considering was isolated, but next, we would like to focus on an open standard map. In such cases, the quantum channel plays an important role. For an open quantum standard map, it becomes important to look into the properties of the

quantum channel associated with it. We will also explore the effect of underlying classical dynamics on the Quantum Channels. In the remaining part of this work, we will look closely at the properties of quantum channels corresponding to the Quantum Standard Map.

Chapter 5

Quantum Channels and Hamiltonian Systems

In theory, we deal with closed quantum systems and the dynamics of which are given by a unitary operator, U . It can be quantum gates operation or a unitary we get from Hamiltonian systems. We are interested in the case when the unitary, U is generated by a Hamiltonian with underlying dynamics. For now, let us not focus on the exact form of U , but we will get back to it later in the chapter.

Pictorially it can be represented as -

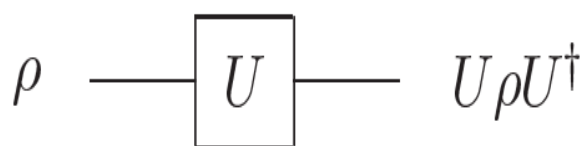


Figure 5.1: The pictorial representation of the unitary transformation of an isolated quantum state. This is taken from ref [29].

In the real world, this situation never occurs. Except for the case when we take our system as the entire universe, we never have close systems. Our systems have some interaction with the outside world, which we call the environment. Such systems are open systems and in principle, we cannot rely on quantum mechanics rules for such systems. These interactions

in real systems are unwanted, and in theory, we often refer to them as noise in our system.

5.1 Quantum Channels

We now consider both environment and system together, which is then a closed system. The rules of quantum mechanics can then be applied in such a setup, and thus, the dynamics of the system environment together are given by unitary transformations. In order to know or study the system, we have to neglect or average the dynamics of the environment. The transformations are then no longer Unitary. This gives rise to the concept of Quantum Channels/Operations/Maps¹.

5.1.1 Completely Positive Trace Preserving Maps

We can transform one state to another via unitary transformations or measurements². But, we can always stop and ask **Is that All?** Can we do anything more? And to state in a clearer way, **What is the most general Quantum Operation to transform one state to another?**

It turns out that a general quantum operation is a special kind of transformation with some definite properties, as we will see. Let \mathcal{E} , denote this general quantum channel/operation. It transforms an input state into an output state as illustrated in Fig.5.2. The unitary and measurement operations are some special forms of this transformation[29]. The output state

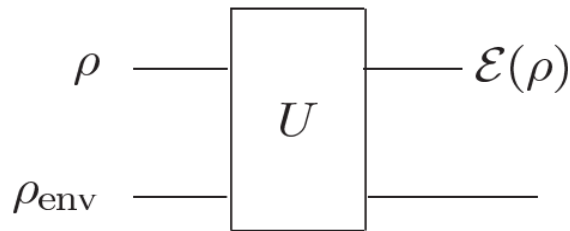


Figure 5.2: A pictorial representation of the evolution of the system in the presence of environment. This is taken from ref [29].

¹We will be sticking to the term Quantum Channel as we reserve Quantum Maps for the quantization of Classical Maps as Quantum Maps.

²Measurement is a non-unitary transformation and causes the collapse of the state in some sense.

is also a valid density matrix, so the properties of the density matrix put some constraint on the quantum channel, \mathcal{E} which are-

$$1. \text{Tr}(\mathcal{E}(\rho)) = \text{Tr}(\rho) = 1 \quad (5.1.a)$$

$$2. \mathcal{E}(\rho) \geq 0. \quad (5.1.b)$$

$$3. (\mathcal{E}_A \otimes (Q_B))(\rho_{AB}) \geq 0. \quad (5.1.c)$$

Here, ρ is the initial state, and $\mathcal{E}(\rho)$ is the state after Quantum Operation. Q represents an arbitrary extension of the system under consideration(here, A) and ρ_{AB} represents the joint state of the system and its extension, B.

From the above three properties, we can say that the channel which represents the most general quantum operation is trace-preserving³, positive and in fact completely positive (property 3). Such quantum channels/operations are known as CPTP or, Completely Positive Trace Preserving Map. Thus, a General **Quantum Channels/Operations is a CPTP map**. There are other ways to look into CPTP maps which we will see in the next sections.

5.1.2 Let's interact!

As we have stated that we have to deal with open systems in the practical world. The system which we want to deal with has some interaction with the environment. We cannot give the dynamics of the system in this case by a unitary on the system alone. Instead, we have to consider system and environment together, which then form a closed system and the evolution of system and environment together is then given by a Unitary, which acts on both system and environment.

Let us consider a system, S initially in the state, ρ_S interacting with an environment E whose state is ρ_E . Also, let us assume that at the beginning, the system and environment are unentangled, and they get entangled by the action of unitary, U_{SE} on the system and environment together. The state of the system and environment after the action of U_{SE} is given as -

$$\rho'_{SE} = U_{SE} (\rho_S \otimes \rho_E) U_{SE}^\dagger \quad (5.2)$$

³In general, it should be trace non-increasing which one can make trace-preserving [28]

ρ'_{SE} is the state of the joint system after a unitary operation. In order to just study the system, we have to find the reduced density matrix of the system, which is then given as -

$$\rho'_S = \text{tr}_E \left(U_{SE} (\rho_S \otimes \rho_E) U_{SE}^\dagger \right) \quad (5.3)$$

This can be written as -

$$\rho'_S = \mathcal{E}(\rho_S) \quad (5.4)$$

where, $\mathcal{E}(\rho)$ is given as -

$$\mathcal{E}(\rho) = \text{tr}_E \left(U_{SE} (\rho \otimes \rho_E) U_{SE}^\dagger \right) \quad (5.5)$$

The operation which we are considering maps a state of a system to another state of a system in a non-unitary fashion. This represents a quantum operation on a system alone in the presence of some environment. .

5.1.3 Operator-Sum Representation and Kraus Operators

We can re-write eq. 5.5 in a much more neat way. This gives rise to another representation known as Operator-Sum Interpretation. It basically says that in such a representation, we can write the quantum operation as an action of some operators, known as Kraus operators[30], which act on the system alone and transform the state of the systems. For simplicity, let the environment be in a pure state, $|0\rangle$ initially. Thus, from eq. 5.5 we have-

$$\mathcal{E}(\rho_S) = \text{tr}_E \left(U_{SE} (\rho_S \otimes |0\rangle\langle 0|) U_{SE}^\dagger \right) \quad (5.6)$$

Now, let the basis of the environment be $\{|e_i\rangle\}$. So, we have -

$$\mathcal{E}(\rho_S) = \sum_i \langle e_i | \left(U_{SE} (\rho_S \otimes |0\rangle\langle 0|) U_{SE}^\dagger \right) | e_i \rangle \quad (5.7)$$

Eq. 5.7 can be written as -

$$\mathcal{E}(\rho_S) = \sum_i E_i \rho_S E_i^\dagger \quad (5.8)$$

where $\{E_i\}$ are known as Kraus operators⁴ and they act on the system. They are given as -

$$E_i = \langle 0 | U_{SE} | e_i \rangle \quad (5.9)$$

⁴Kraus operators are not unique. For a detailed understanding of Kraus operators, one may look at the book by Kraus[30]. It contains references to earlier works.

Also, the state of the system after the quantum operation is then given as -

$$\rho'_S = \sum_i E_i \rho_S E_i^\dagger \quad (5.10)$$

Since both ρ'_S and ρ_S are valid density matrices, the trace should be one for both. That is,

$$\text{Tr}(\sum_i E_i \rho_S E_i^\dagger) = 1 \quad (5.11)$$

Now, due to the cyclic properties of Trace, we get-

$$\sum_i E_i^\dagger E_i = 1 \quad (5.12)$$

We have shown in the appendix C that-

$$\mathcal{E}(\rho) \geq 0 \quad (5.13.a)$$

$$(\mathcal{E}_{\mathcal{A}} \otimes Q_B)(\rho_{AB}) \geq 0 \quad (5.13.b)$$

Therefore, $\mathcal{E}(\rho)$ is a CPTP map. Using operator-sum representation, we have actually shown that a Unitary Transformation of the system and environment together is actually a CPTP map on the system alone. This gives a nice physical motivation to the CPTP maps.

There are many interesting things about CPTP maps, which we haven't covered but any interested reader can look them up in [28] or [30] and also in other standard books on Quantum Information Theory.

5.1.4 Superoperator Representation

Superoperators are nothing but operators which act in the vector space of linear operators. The vectors of linear operators are nothing but vectorization of the operators. An operator A can be represented by a matrix whose elements are given as -

$$A_{ij} = \langle i | A | j \rangle \quad (5.14)$$

. The vectorization of operator A is then defined as-

$$\langle i | A | j \rangle = \langle ij | A \rangle \quad (5.15)$$

After vectorization, the operator A can be represented as a state vector, $|A\rangle$. A general quantum operation needs to satisfy the properties given by eq. 5.1. The authors Sudarshan, Mathews, and Rau in [31] constructed the most general quantum dynamical operation based on these three properties as given by eq. 5.17.

Let us consider a system-environment setup with an environment in the maximally mixed state, i.e., $\rho_E = I_E/d$. Let us choose the basis $\{|i\rangle\}$ and $\{|\alpha\rangle\}$ for the system and environment respectively. Thus, a matrix element form of eq. 5.3 can be written as -

$$\langle i|\rho'_S|j\rangle = \sum_{\alpha} \langle i\alpha| \left(U_{SE} (\rho_S \otimes \frac{I}{d}) U_{SE}^{\dagger} \right) |j\alpha\rangle \quad (5.16)$$

We have shown in the appendix D that on simplification, we get-

$$|\rho'_S\rangle = M(|\rho_S\rangle) \quad (5.17)$$

where, $|\rho\rangle$ is the vectorization of ρ and M is the quantum channel whose form is -

$$M(U) = \frac{1}{d} (U^{R_2} (U^{R_2})^{\dagger})^{R_1} \quad (5.18)$$

here, R_1 and R_2 are the realignment operation and in some sense, it is a reshuffling of the entries of the matrix in a particular way, Appendix D. Since we had a CPTP channel thus, M is also trace-preserving and completely positive. There is also a notion of a complementary channel, M_c for the channel, M . It is obtained by first swapping the system and environment using Swap Operators, S and then tracing out the 1st subsystem(which now is environment due to swap). This gives a state in the environment space and not in the system space. Thus, the complementary channel takes the state of the system to another state in the environment space. On the other hand, channel, M takes the state of the system to another state of the system itself. The transformation for the quantum channel, M_c is given as -

$$\sigma = Tr_S \left[U_{SE} S.S \left(\rho_S \otimes \frac{I}{d} \right) S.S U_{SE}^{\dagger} \right] \quad (5.19)$$

where, $S|\psi_1\rangle|\psi_2\rangle = |\psi_2\rangle|\psi_1\rangle$ and we can see, $S.S = I$. We have used this property in writing eq. 5.19. The state after the operation is given as-

$$|\sigma\rangle = M_c|\rho_S\rangle \quad (5.20)$$

where, M_c is given as -

$$M_c(U) = \frac{1}{d} (U^{T_2} (U^{T_2})^\dagger)^{R_1} \quad (5.21)$$

Here, U^{T_2} is partial transpose on subsystem two, and similarly, we can define partial transpose on subsystem 1. Just like realignment, they are also some reshuffling of the matrix but in a different way, Appendix D. The form M_c is derived in appendix D. Also,

$$M_c(U) = M(SU) \quad (5.22)$$

Some points to Note:

- For $U=\text{unitary}$, U_{R_i} , $i=\{1,2\}$, may or may not be Unitary.
- When U_{R_2} is also unitary, then U is known as a dual unitary operator.
- When $U_{T_2} \in \mathcal{U}_d$ then, U is T-dual. Here, \mathcal{U}_d is a space of unitary matrix with dim, d.
- If both U_{R_2} and U_{T_2} is unitary then, U is known as 2-unitary.
- The channel, M , is an unital channel if the most mixed state, I/d , is unchanged by its operation. i.e.,

$$M(I/d) = I/d \quad (5.23)$$

Depolarizing Channel:

When U is dual unitary then, $M(U)$ is nothing but a realignment of I/d , i.e.,

$$M = \frac{1}{d} (I)^{R_1} \quad (5.24)$$

It is easy to check that,

$$\frac{(I)^{R_1}}{d} = |\phi^+\rangle\langle\phi^+| \quad (5.25)$$

where, $|\phi^+\rangle$ is one of the bell state, and $|\phi^+\rangle\langle\phi^+|$ is the projector onto the bell state. Thus, the channel takes any state of the system, S and projects it to the maximally mixed state, I/d . Hence, in this case, M acts as a perfect Depolarizing Channel. A similar, argument holds for the complementary channel, M_c , when U is T-dual.

5.2 Quantum Channel for Hamiltonian Unitary

We will like to get back to Hamiltonian Systems not just because we love them but because they are quite common and have interesting properties. We have seen before that we get the unitary associated with a Hamiltonian system can be obtained by exponentiation of the Hamiltonian, H . When the Hamiltonian system is chaotic, the eigenstates of U and also entanglement have some unique features which are different when the system is integrable, sec. 4.4.

Quantum channels, on the other hand, also include the unitary and whose behaviour might vary with the properties of U . This motivated us to look into the properties of Quantum Channels as a function of U and also to find some trademark of chaos if any exists. Since we were looking at Quantum Standard Map, we would take this unitary, U_{SE} , which acts on the system-environment together as the unitary associated with the standard map defined in 4.2.6. The form of this unitary is -

$$U = (U_1 \otimes U_2) U_b \quad (5.26)$$

We now treat one of the kicked pendulums as the environment and the other as the system. U_1 and U_2 then correspond to local operations on the system and environment, whereas, U_b is the interaction between the two. In general, the dimension of the environment can be anything, and it can go to as large as ∞ , but, in our case, the dimension of the environment is the same as that of the system.

Complementary Channel

U_b , which denotes the interaction between the system and environment, is diagonal. It has been shown that diagonal matrices are T-dual,i.e, $U_b^{T_2}$ is unitary and thus, U^{T_2} is also unitary as U_1 and U_2 are local unitaries. Hence, M_c as defined in eq.5.21 acts as a perfect depolarizing channel in the case of the unitary of a standard map. Therefore, for the unitary, U corresponding to the quantum standard map, the non-trivial channel is M . We would go deep into looking at various properties of M , like eigenvalues, norms, etc., in the next chapter.

Chapter 6

Spectral Properties of Quantum Dynamical Channels

In the previous chapter, we have introduced the concept of open systems and quantum channels. We have also introduced the idea of using the unitary for the coupled standard map. Here, in this case, one pendulum is our system, and the other acts as an environment, and Unitary, U is the same as introduced in sec.[4.2.6](#). The form of the Unitary, U is -

$$U = (U_1 \otimes U_2) U_b \quad (6.1)$$

where U_b is responsible for the interaction between the system and the environment.

As derived in Appendix [D](#), the corresponding channel, M is -

$$M(U) = \frac{1}{d} (U^{R_2} (U^{R_2})^\dagger)^{R_1} \quad (6.2)$$

It is known for a long time that the underlying classical chaos and integrability have slightly different quantum properties, and also periodic orbit scars the quantum eigenstates in case of complete chaos. Our interest is to study the spectral properties of this channel to find what effect underlying chaos has on it and also to find scarring of eigenvectors, if there is any. There are various parameters like K_1 , K_2 , b and N on which U depends. Hence our channel, M , will also depend on these parameters.

This chapter is mainly presenting various results we have obtained and which we ourselves

are trying to understand. We still lack a strong theoretical background supporting our results.

6.1 Operator Entanglement

We have defined what entanglement for states means, and now we will look at Entanglement for operators.

Let U be a unitary operator acting on a bipartite space, \mathcal{H}^{AB} , where $\mathcal{H}^{AB} = \mathcal{H}_N^A \otimes \mathcal{H}_N^B$. The vectors in \mathcal{H}^{AB} are operators, and hence, \mathcal{H}^{AB} is the Hilbert space of operators. Unless U is of product form ($U_A \otimes U_B$), it creates entanglement between two unentangled states. U is a vector in \mathcal{H}^{AB} so we can write its Schmidt decomposition as -

$$U = \sum_{k=1}^{N^2} \sqrt{\gamma_k} M_k \otimes L_k \quad (6.3)$$

where, M_k and L_k forms an orthonormal basis for the operators in \mathcal{H}^A and \mathcal{H}^B respectively. Taking $\text{Tr}(UU^\dagger)$ one can show that-

$$\sum_{k=1}^{N^2} \frac{\gamma_k}{N} = 1 \quad (6.4)$$

Thus, just like in the Schmidt decomposition of states, the sum of all Schmidt coefficients adds up to 1. We can define the probability, p_k as -

$$p_k = \frac{\gamma_k}{N} \quad (6.5)$$

Hence, we can now define linear entropy[28] for operators as we have for states as-

$$E(U) = 1 - \frac{1}{N^4} \sum_{j=1}^{N^2} (\gamma_j)^2 \quad (6.6)$$

How to find γ_k ?

Realigning¹ the operator, U we get -

$$U^{R_2} = \sum_{k=1}^{N^2} \sqrt{\gamma_k} |M_k\rangle\langle L_k^*| \quad (6.7)$$

¹It is discussed in appendix D

Now, when we take the hermitian conjugate of the above eq., we get -

$$(U^{R_2})^\dagger = \sum_{k=1}^{N^2} \sqrt{\gamma_k} |L_k^*\rangle \langle M_k| \quad (6.8)$$

Multiplying the two, we get-

$$U^{R_2}(U^{R_2})^\dagger = \sum_{k=1}^{N^2} \sqrt{\gamma_k} |M_k\rangle \langle M_k| \quad (6.9)$$

Hence, γ_k are the eigenvalues of matrix $U^{R_2}(U^{R_2})^\dagger$. Therefore,

$$\sum_{k=1}^{N^2} (\gamma_k) = \text{tr} \left[(U^{R_2}(U^{R_2})^\dagger)^2 \right] \quad (6.10)$$

Now, we can rewrite eq. 6.6 as -

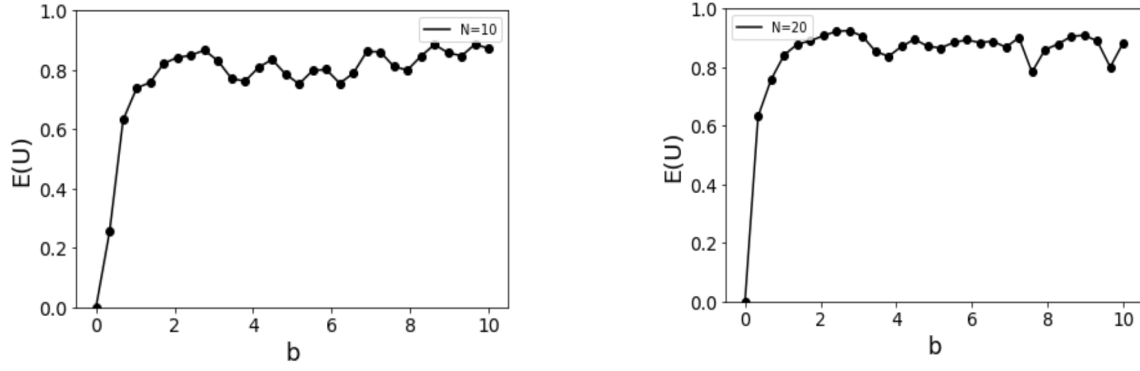
$$E(U) = 1 - \frac{1}{N^4} \text{tr} \left[(U^{R_2}(U^{R_2})^\dagger)^2 \right] \quad (6.11)$$

When U is of the form, $U_1 \otimes U_2$, then there will be no interaction between the system and environment and hence, $E(U) = 0$. Also, $E(U)$ is maximum when $(U^{R_2}(U^{R_2})^\dagger)^2$ is I , which is the case when U is dual unitary operator, i.e., U^{R_2} is also unitary. Thus,

$$0 \leq E(U) \leq 1 - \frac{1}{N^2} \quad (6.12)$$

The operator entanglement, in a way, will quantify the amount of entanglement U is capable of creating between the system and the environment. Hence, $E(U)$ should only depend on b , which is the coupling constant and not on local variables, K_1 and K_2 . The variation of this quantity with b is depicted in Fig.6.1. From the figure, we conclude that -

- For $b=0$, $E(U)=0$.
- For $N = 10$, the saturation value is nearly 0.75 and for $N = 20$ is nearly 0.88 and which is less than $1-1/N^2$ in both cases, as U is not dual unitary.
- The dips are reducing as we increase N .


 (a) $E(U)$ vs b for $K_1=0.1, K_2=0.2$ and $N=10$

 (b) $E(U)$ vs b for $K_1 = 0.1, K_2 = 0.2$ and $N = 20$

Figure 6.1: The variation of operator entanglement, $E(U)$ as we change the coupling parameter, b which controls the interaction between system and environment

- The saturation is attained faster for $N = 20$ than $N = 10$.

The above results are in agreement because as we increase N , the dimension of both the system and the environment increases, and interactions are capable of creating more entanglement between the two. But, entanglement can never reach the maximum value even if we increase the N further because U is not dual-unitary.

Next, we will like to look at the norm of the superoperator of the channel, M . We will see how the norm of M is related to $E(U)$.

6.2 Norm of the channel, M

There are various norms of a matrix. But, we will be using Hilbert-Schmidt or Frobenius norm, which is defined as-

$$\|M\|^2 = \text{tr} (MM^\dagger) \quad (6.13)$$

From eq. 6.2 let-

$$M = \frac{1}{N}(M_1)^{R_1} \quad (6.14)$$

where, $M_1 = U^{R_2}(U^{R_2})^\dagger$.

Using the identity $(A^{R_1})^\dagger = (A^\dagger)^{R_2}$ it is easy to show that -

$$\|M\|^2 = \frac{1}{N^2} \text{tr} \left[(U^{R_2} (U^{R_2})^\dagger)^2 \right] \quad (6.15)$$

Thus,

$$\|M\|^2 = [1 - E(U)] N^2 \quad (6.16)$$

Since, $E(U)$ is bounded, the bound on $\|M\|^2$ is -

$$1 \leq \|M\|^2 \leq N^2 \quad (6.17)$$

where, $\|M\|^2 = N^2$ when $E(U) = 0$ and 1 when $E(U)$ is maximum which is for dual unitary operator, U .

6.3 Spectral Properties

The spectrum of eigenvalues of the superoperator, M , helps us to understand the evolution of the open quantum system[32]. Thus, it is important to look closer at the spectral properties of the channel. Also, it has been shown in ref [33] that for an open Baker's map, the spectrum of the superoperator follows a universal feature in the case of complete chaos. They employ a different approach from what we are using. Hence, the underlying chaotic and integrable cases have different impacts on the spectrum, and we will like to investigate them in more detail.

6.3.1 Relation between Eigenvalues, $\|M\|^2$ and $E(U)$

The operator, M is non-hermitian, and it might not be possible to diagonalize such matrices hence, it is first not clear how to relate the eigenvalues of M and $\|M\|^2$. However, there exists another decomposition that simplifies the situation in such cases, known as Schur Decomposition[34]. It states that-

Theorem 1: For any $n \times n$ matrix with entries from complex space, \mathcal{C} , there is some orthonormal basis V of \mathcal{C} and some upper-triangular matrix, T with entries in \mathcal{C} such that -

$$A = V T V^\dagger \quad (6.18)$$

where V is unitary.

The form in eq. 6.18 is very similar to that of diagonalization except for the fact that here, T is not a diagonal matrix but instead an upper triangular matrix. We can decompose our superoperator, M using Schur decomposition, and one can easily verify that -

$$\|M\|^2 = \|T\|^2 \quad (6.19)$$

This is true because V is a unitary matrix, and when we take hermitian conjugate to define the norm, VV^\dagger becomes Identity.

The diagonal entries of T are the eigenvalues of M counted with the degeneracy and,

$$\|T\|^2 \geq \sum_{i=0}^{N^2-1} |\lambda_i|^2 \quad (6.20)$$

where, $\{\lambda_i\}$ are the eigenvalues of M .

Now, from eq. 6.19 we have-

$$\sum_{i=0}^{N^2-1} |\lambda_i|^2 \leq \|M\|^2 \quad (6.21)$$

This can be seen in Fig. 6.2

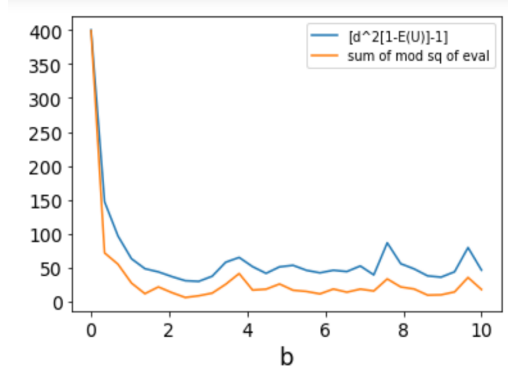


Figure 6.2: The variation of $\sum_{i=0}^{N^2-1} |\lambda_i|^2$ and $\|M\|^2$ with b . The bound given by eq.(6.21) is satisfied.

Just like, there is a bound of $\|M\|^2$ as given in eq. 6.17 we have -

$$1 \leq \sum_{i=1}^{N^2} |\lambda_i|^2 \leq N^2 \quad (6.22)$$

- Case 1: $\sum_{i=1}^{N^2} |\lambda_i|^2 = 1$

When U^{R_2} is unitary, the channel acts as a completely depolarizing channel, as explained in sec 5.1.4. Given this scenario, channel M will have just one eigenvalue, $\lambda_1 = 1$, and all others will be zero.

- Case 2 : $\sum_{i=1}^{N^2} |\lambda_i|^2 = N^2$

This is the case when $U = U_1 \otimes U_2$. In that case, the channel M is -

$$M = U_1^\dagger \otimes U_1^T \quad (6.23)$$

Hence, M is also unitary and therefore, the eigenvalues will lie on a unit disk as illustrated in Fig. 6.3 in the complex plane. Thus, $|\lambda_i| = 1 \forall i=\{1,N^2\}$ and hence sum of all those will be N^2 .

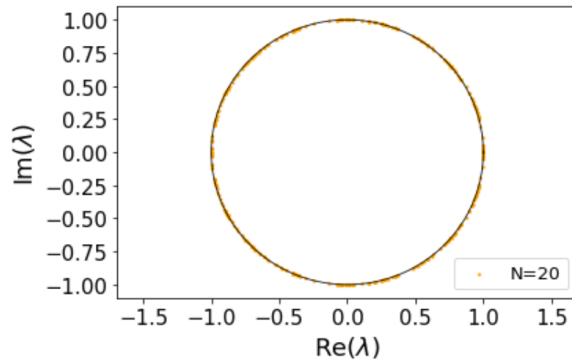


Figure 6.3: Eigenvalue Distribution of Channel, M for $b = 0, N = 20, K_1 = 1.0, K_2 = 1.1$. lies on a unit circle in complex plane.

6.3.2 Important features of channel and their impact on eigenvalue spectrum

- **Unital Channel:**

An unital channel is the one which leaves the most mixed state invariant. That is-

$$M|\rho\rangle = |\rho\rangle \quad (6.24)$$

where $|\rho\rangle = I/d$.

Thus, for such a channel, $\lambda = 1$ is the largest trivial eigenvalue. The spectral radius[34] is then 1, and all the eigenvalues lie inside the unit disc on the complex plane.

We can then define the peripheral spectrum, as defined in ref [34], as a set of eigenvalues with a magnitude equal to the spectral radius. Any initial state then approaches this peripheral eigenspace by the repetitive action of the channel, M . From the eigenvalue distribution of $M(U)$, Fig. 6.4 and we can say that the channel which we are interested in is also Unital, and hence, any initial state will eventually converge to the maximally mixed state, I/d as shown in Fig.6.5.

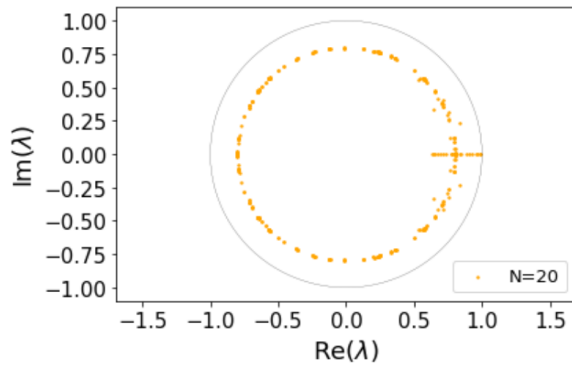


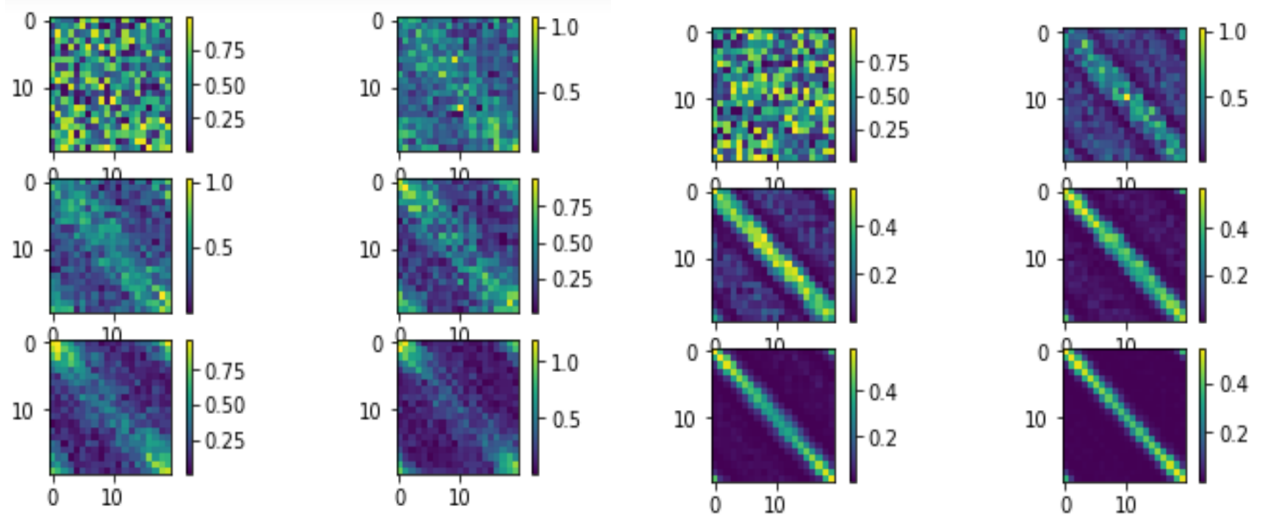
Figure 6.4: Eigenvalue Distribution of M for $N = 20$, $K_1 = 0.1$, $K_2 = 0.2$, $b = 0.2$. There is an eigenvalue 1 on the unit circle.

The detailed study of the variation in eigenvalue distribution is reserved for later. Here, we just intended to show that there is a trivial eigenvalue and all other eigenvalues are less than that. From now on, we will be looking at the spectrum of non-trivial eigenvalues, i.e., the set of eigenvalues except the eigenvalues 1.

Action of Map, M on a random initial state:

We have said earlier that any random state will converge to the peripheral eigenspace with repeated action of the channel, M . So, we take a random initial state and apply the channel on it five times. The convergence to the peripheral eigenspace is clear from Fig. 6.5, but the rate of convergence depends on the interaction strength, b , between the system and the environment. As we increase b further, the convergence will be much faster. This depicts the decoherence phenomenon. It has been presented in ref [35] that a general quantum channel shows exponential convergence to this peripheral

eigenspace(which is I/d for an unital channel), and the rate of convergence depends on the spectral gap, which is the difference between the moduli of two largest eigenvalues. From fig. 6.4 and 6.3, it is somewhat clear that the spectral gap changes with b , and thus, we get different rates of convergence for different b as we observe.



(a) For $K_1 = 0.1, K_2 = 0.2, b = 0.2$ and $N = 20$ (b) For $K_1 = 0.1, K_2 = 0.2, b = 0.6$ and $N = 20$

Figure 6.5: The action of the channel, M on a random initial state. We can see that the state is converging to I/d .

- **Hermiticity Preserving Channel:**

If for a channel

$$M|\mathcal{X}^\dagger\rangle = (M|\mathcal{X}\rangle)^\dagger \quad (6.25)$$

then the channel is known as Hermiticity preserving channel[32], i.e., a hermitian operator is hermitian even after the action of the channel.²

For the form of M as -

$$M(U) = \frac{1}{d} (U^{R_2} (U^{R_2})^\dagger)^{R_1} \quad (6.26)$$

$M(U)$ is a Hermiticity preserving channel as it is a CPTP channel and takes a positive operator to a positive operator. Let us see what is the effect of this property on the

²Here, \mathcal{X} is an operator, but it is a vector for the superoperator M . We are in the Hilbert space of operators where operators are vectors. That is why M is a superoperator, an operator in operator space.

eigenvalue spectrum. The eigenvalue equation of M is-

$$M|\mathcal{Y}\rangle = \lambda|\mathcal{Y}\rangle \quad (6.27)$$

where, $|\mathcal{Y}\rangle$ is the eigenvector corresponding to eigenvalue, λ . Since it is a hermiticity-preserving map, due to eq. 6.25 we have-

$$M|\mathcal{Y}^\dagger\rangle = \lambda^*|\mathcal{Y}^\dagger\rangle \quad (6.28)$$

Thus, $|\mathcal{Y}^\dagger\rangle$ is also a eigenvector of M corresponding to the eigenvalue λ^* . The case when $\mathcal{Y} = \mathcal{Y}^\dagger$, $\lambda = \lambda^*$. Therefore, the eigenvalues of M are either purely real or are complex conjugate pairs, as for every λ , λ^* is also an eigenvalue. This can be seen from Fig. 6.4

6.3.3 Variation of eigenvalue distribution:

We have stated that the eigenvalue of the M will lie inside a unit circle in a complex plane. M is a function of the unitary, U , which for a standard map depends on various parameters like K_1 , K_2 , N and b . The eigenvalues distribution of M thus will also depend on these parameters, and we will like to examine this variation for different cases closely.

- **Changing K_1, K_2, b and N :**

- **For low K_1, K_2 and varying b and N :**

We have taken the value of $K_1 = 0.1$ and $K_2 = 0.2$

* Case 1: $b = 0.05$ and $N = 20$ and 40 :

For $b = 0$, U is a unitary matrix, and so is M . So, the eigenvalues of M will lie on a unit circle in the complex plane, as shown in fig.6.3. As we increase b , M becomes non-unitary, and eigenvalues are no longer on the unit circle. But, we observe, as in fig.6.6 (a) and (b), that the eigenvalues are still nearly on the unit circle for $N = 20$. They have shifted slightly from the unit circle. However, for $N = 40$, the eigenvalues no

6.3. SPECTRAL PROPERTIES

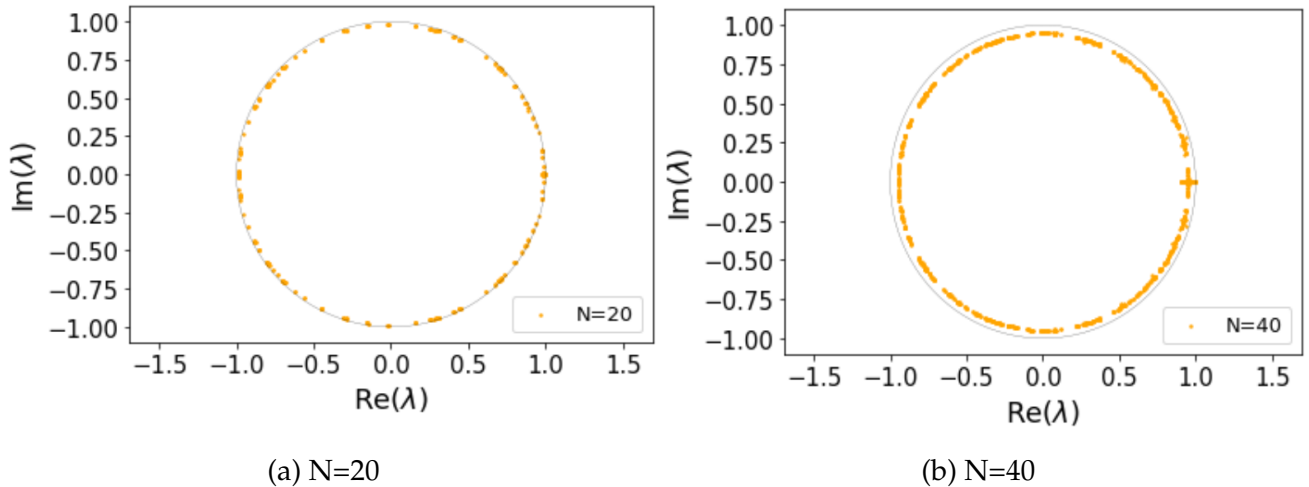


Figure 6.6: Eigenvalue distribution of M with $b = 0.05$, $K_1 = 0.1$ and $K_2 = 0.2$

longer lie on the unit circle except few real eigenvalues. Thus, the amount with which the circle moves depend on N for fixed other parameters.

Another observation is that there are few eigenvalues that are purely real. The trivial eigenvalue of the superoperator, M , is 1, which is not included in the figure. The largest non-trivial eigenvalue is real and has a value close to 1. The number of real eigenvalues is more as we increase N as the eigenvalues themselves increase.

* Case 2: $b = 0.1$ and for $N = 20$ and 40 :

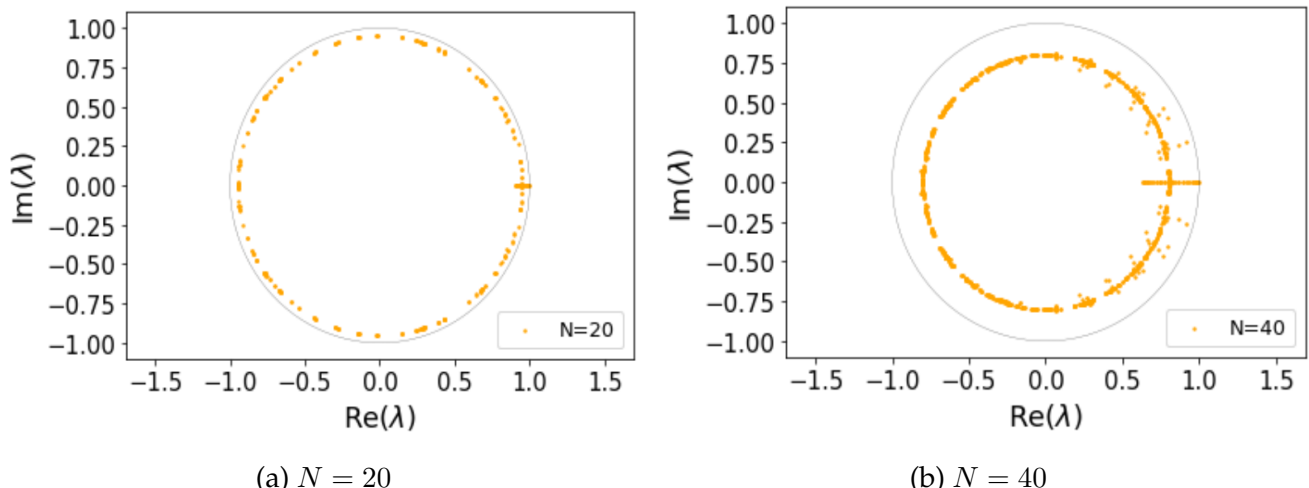


Figure 6.7: Eigenvalue distribution of M with $b = 0.1$, $K_1 = 0.1$ and $K_2 = 0.2$

As we have increased b to 0.1, as compared to case 1, we observed that the radius of the circle on which eigenvalues lie has shrunk now, even for $N = 20$ and again, the amount with which the circle moves inside depends on N . Also, the real line corresponding to purely real line values has increased.

* Case 3: $b = 0.5$ and $N = 20, 30$ and 40 :

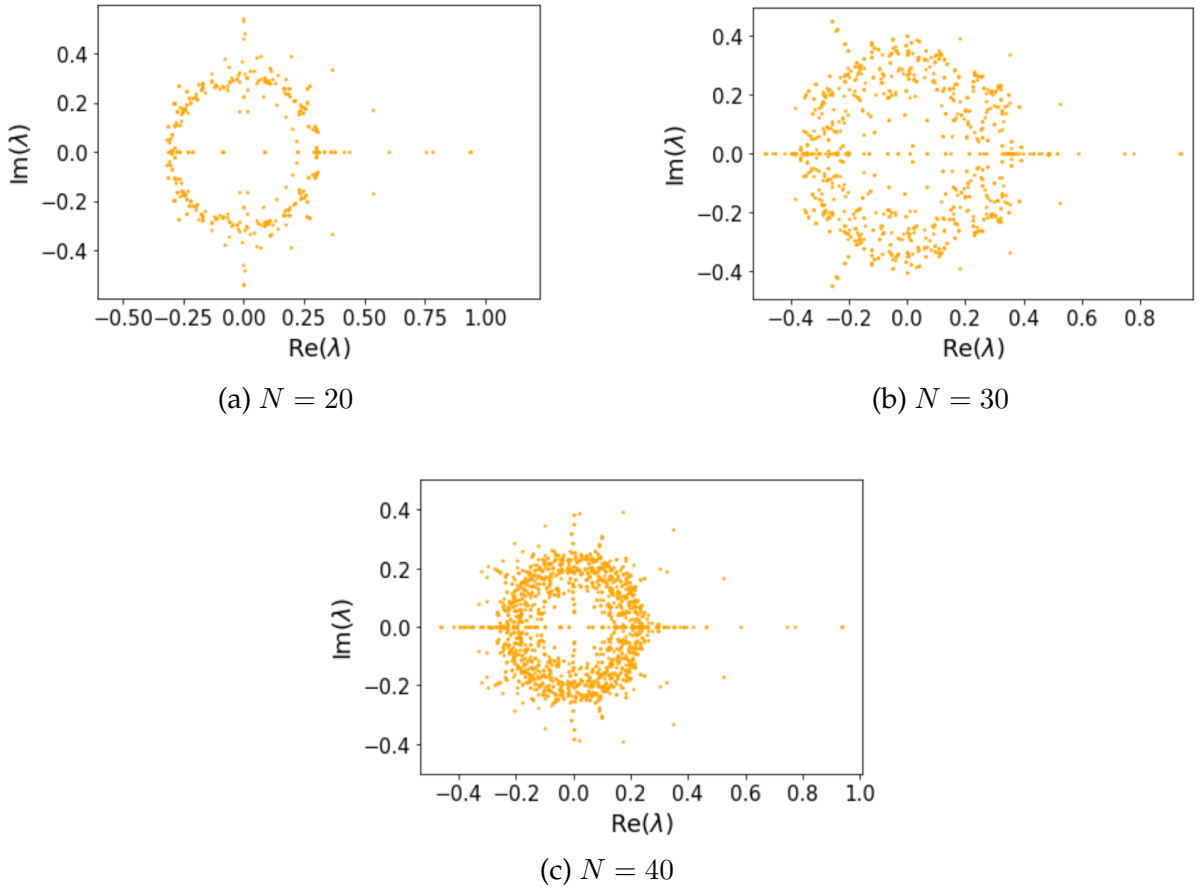


Figure 6.8: Eigenvalue distribution of M with $b = 0.5$, $K_1 = 0.1$ and $K_2 = 0.2$

For $b = 0.5$, as illustrated in Fig. 6.8, the radius of the circle on which the eigenvalues lie has decreased. The number of real eigenvalues has increased. For $N = 20$ and 40 as in Fig.6.8 (a) and (c), there is yet another line with eigenvalues that are purely imaginary. The purely imaginary line is, however, missing in the case when $N = 30$, Fig.6.8 (b). Also, we observe that the eigenvalues are now not just on the boundary of the circle but are also spreading more inside the circle as we increase N . The eigenvalue

distribution now forms a structure of a ring. Also, when we look at Fig. 6.8 (b) and (c), the eigenvalues for the former, $N = 30$ are much more spread than the latter case, $N = 40$.

* Case 4: $b = 1.0$ and $N = 20, 30$ and 40 :

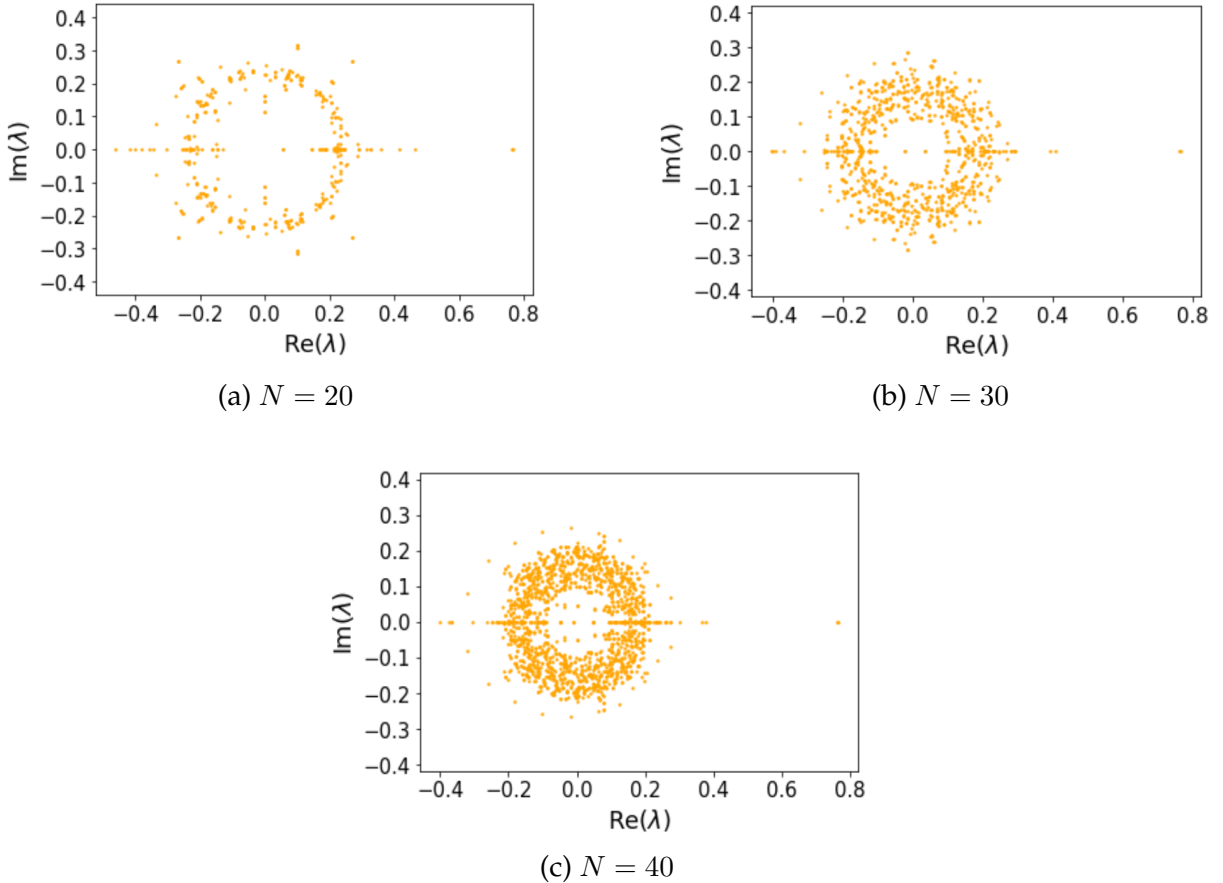


Figure 6.9: Eigenvalue distribution of M with $b = 1.0$, $K_1 = 0.1$ and $K_2 = 0.2$

Fig.6.9 represents the eigenvalue distribution for this case. An annular structure is still present, as was in the previous case. The purely imaginary line which appeared in the previous case for $N = 20$ and $N = 40$ seems to be absent in this case, but few purely imaginary eigenvalues seem to be still present. When we compare the eigenvalue distribution for $N = 30$ with the previous case, case 4, we observe that the eigenvalues are less spread and also lie in an annular region. The outer and inner radius of the annular region decreases for $N = 40$, as compared to the previous case. We can see

that the inner radius has shrunk more than the outer radius.

* Case 5: $b = 2.0$ and $N = 20, 30$ and 40 :

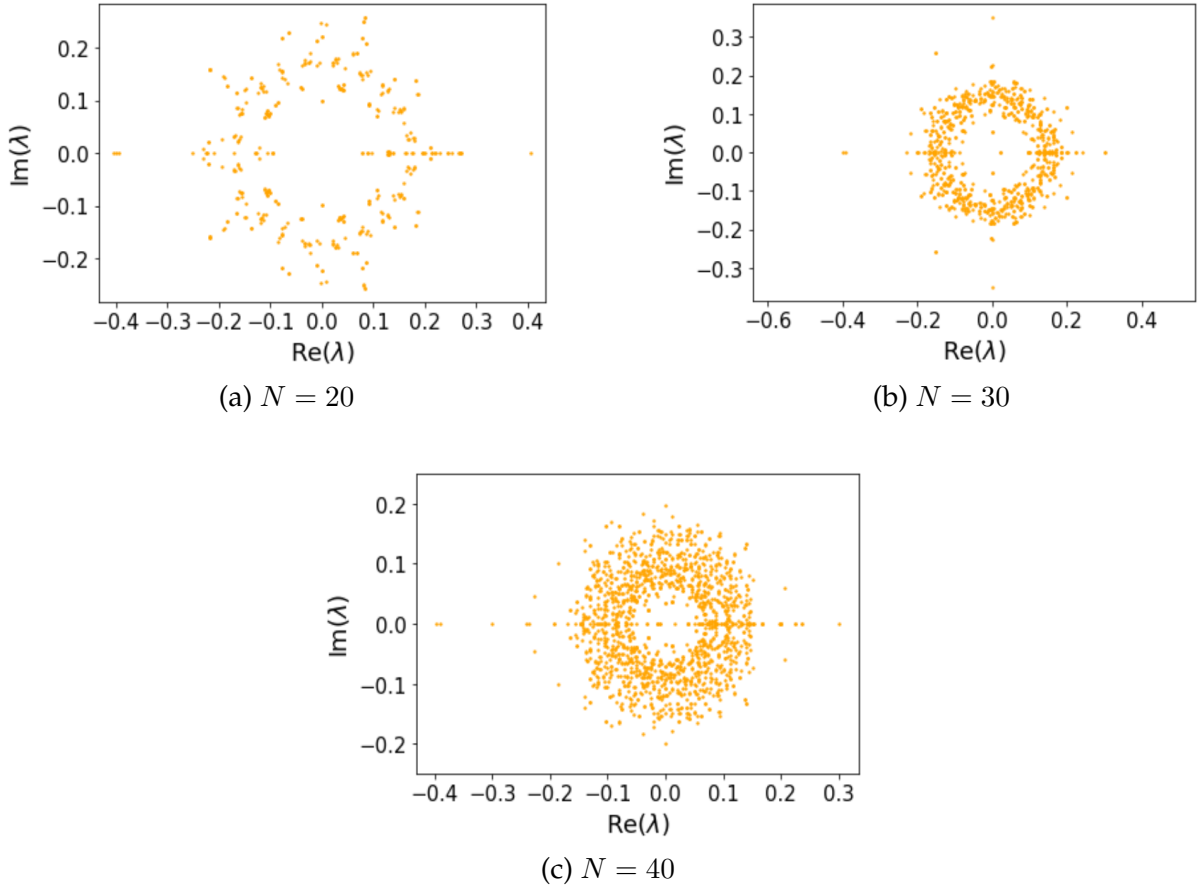


Figure 6.10: Eigenvalue distribution of M with $b = 2.0$, $K_1 = 0.1$ and $K_2 = 0.2$

The interaction between the system and the environment is very large when $b = 2$. The eigenvalue distribution is then given in Fig. 6.10. We observe a purely imaginary line for $N = 30$, which was previously present in the case of $N = 20$ and $N = 40$ when b was 0.5. The real eigenvalue line, however, is still present. The largest non-trivial eigenvalue is now much farther away from 1. The annular region is still there, but the hole is shrinking.

We have looked at the variation eigenvalue distribution of $M(U)$ with b and N for $K_1 = 0.1$ and $K_2 = 0.2$. The above five cases can be summarized as follows -

- The eigenvalue distribution continues to lie on a circle with a radius less than unity for $b = 0.05$ and $b = 0.1$. The largest non-trivial eigenvalue is close to 1. There are, however, few purely real eigenvalues that increase in number as we increase N or b .
- The circle on which eigenvalues lie starts moving inside the unit circle as we increase b for other parameters fixed. But, also, when we look at the eigenvalue distribution for different N with fixed other parameters, the extent to which the circle has moved inside increases as we increase N .
- As we increase b further, the circle starts to shrink, and in fact, now the eigenvalues form a ring. The real eigenvalues are still present, and their number has increased.
- There are a few cases i.e., for some value of b , we also get purely imaginary eigenvalues in addition to the purely real eigenvalue. But, unlike real eigenvalues, they appear only in some cases.
- There are degeneracies in the eigenvalues.

So far, we have just looked at the case when K_1 and K_2 are small. A single classical standard map for small K_1 and K_2 is nearly integrable. Now, we would like to examine the case when K_1 and K_2 is such that the single classical standard map has mixed phase space, and thus there is chaos along with regions of regular islands. By doing so, we wish to study the effect of chaos present in the local system on the eigenvalues of the superoperator M , again as we vary b .

– **For high K1,K2 and varying b and N:**

We take $K_1 = 4.5$ and $K_2 = 4.0$. The phase space of the classical standard map, in this case, is mixed. There is chaos in some regions of the phase space.

* Case 1: $b = 0.05$ and $N = 20$ and 40

The eigenvalue distribution in fig.6.11 looks similar to the case in fig.6.6. The radius of the circle is the same for low K_i and high K_i . However, the distinction is in the number of distinct eigenvalues or in the degeneracies in the eigenvalues. In fig.6.6,

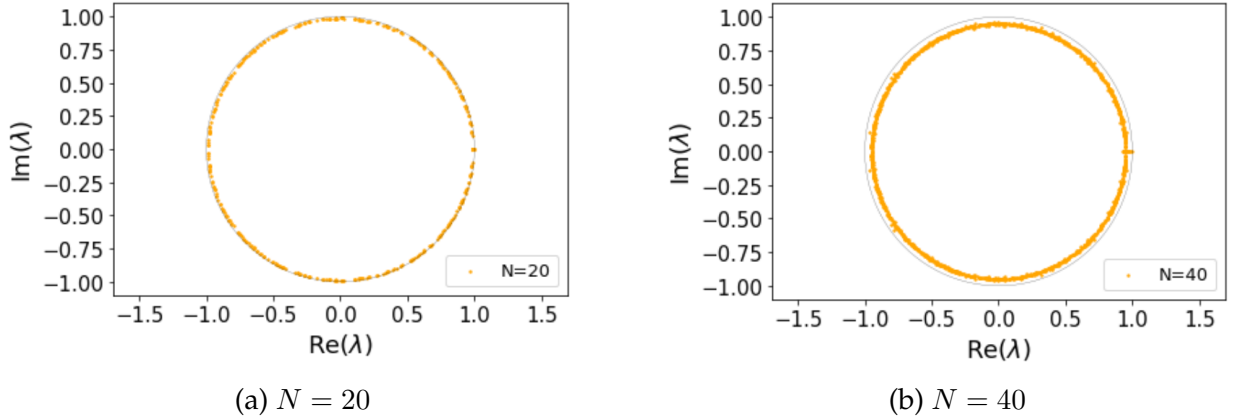


Figure 6.11: Eigenvalue distribution of M with $b = 0.05$, $K_1 = 4.5$ and $K_2 = 4.0$

we observe fewer eigenvalues as compared to fig.6.11 for the same N . Thus, we can say that the degeneracy of some of the eigenvalues is lifted when we increase K . For $N = 40$, fig. 6.11 (b), we see that the circle has a little spread and is more of a ring with a small difference between the inner and outer radius, unlike the case when K_i was small, fig.6.6 (b)

* Case 2: $b = 0.1$ and $N = 20$ and 40

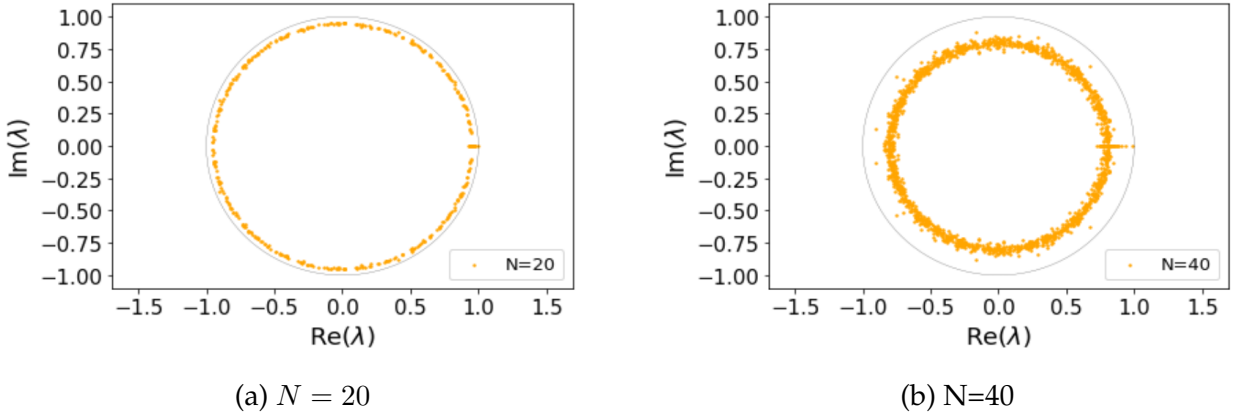


Figure 6.12: Eigenvalue distribution of M with $b = 0.1$, $K_1 = 4.5$ and $K_2 = 4.0$

* Case 3: $b = 0.5$ and $N = 20$ and 40

Similarly, when we compare the eigenvalue distribution for low K_i and high K_i for case 2 and case 3, we observe that the eigenvalues are more spread inside the circular

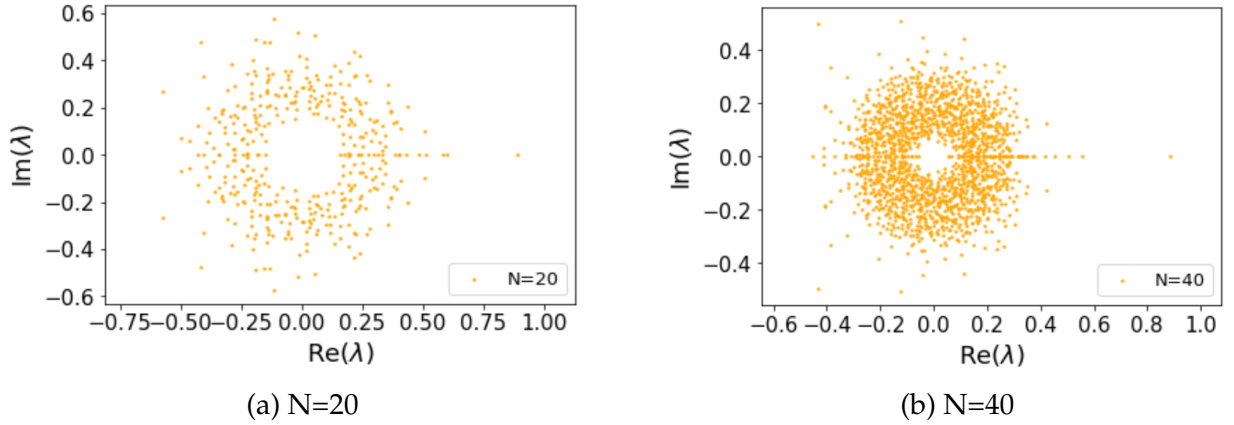


Figure 6.13: Eigenvalue distribution of M with $b = 0.5$, $K_1 = 4.5$ and $K_2 = 4.0$

region, and the line of real eigenvalues is still present. For the case when $b = 0.5$, in case 3, we observed a few purely imaginary eigenvalues for low K , fig. 6.8 (a) and (c), but for high K , there is no such line of purely imaginary eigenvalues.

Also for $N = 20$ and $b = 0.5$ with $K_1 = 0.1$ and $K_2 = 0.2$, we do not get an annular region which we get for $K_1 = 4.5$ and $K_2 = 4.0$. For $N = 40$, the area of the hole in the disk is more for low K_i when compared to the case of large K_i .

* Case 4: $b = 1.0$ and $N = 20$ and 40

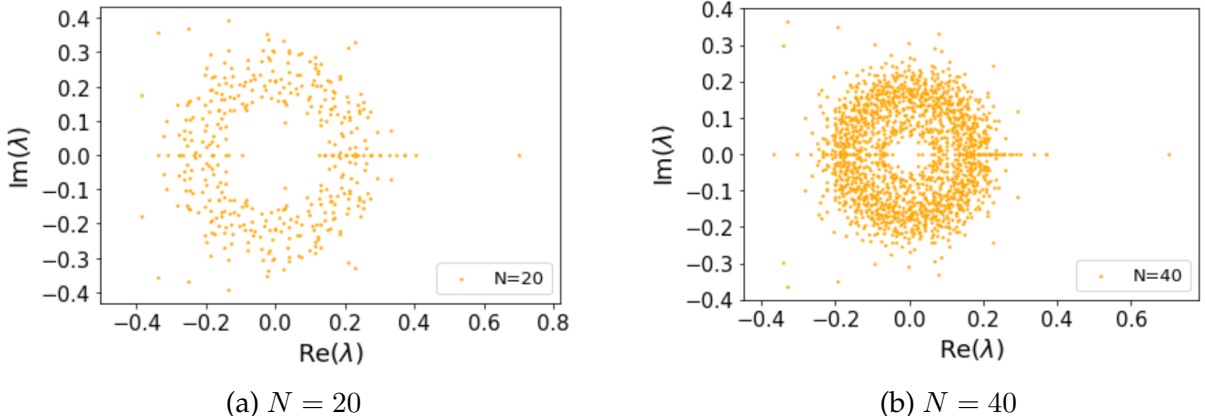


Figure 6.14: Eigenvalue distribution of M with $b = 1.0$, $K_1 = 4.5$ and $K_2 = 4.0$

* Case 5: $b = 2.0$ and $N = 20$ and 40

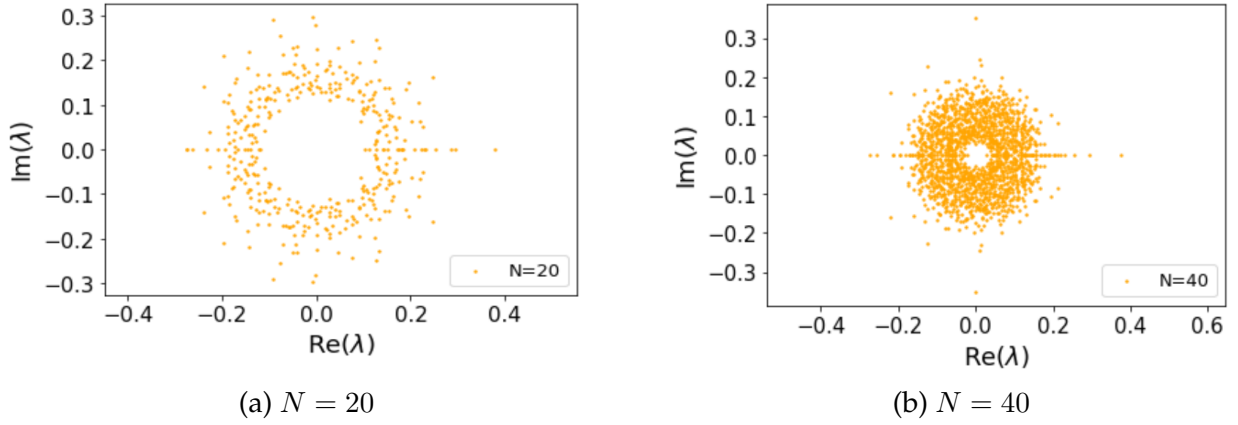


Figure 6.15: Eigenvalue distribution of M with $b = 2.0$, $K_1 = 4.5$ and $K_2 = 4.0$

Similar observations hold for case 4 and case 5 as in the previous cases. For $N = 40$ in the two cases, we can see that the eigenvalue distribution is turning into a ring with the area of the hole getting smaller.

We can thus say that K_i controls the degeneracy of the eigenvalues. As the degeneracy in the eigenvalues is lifted, the eigenvalues are much more spread inside the outside larger circle, and the spread is more for larger N . The area of the annular region for high K_i is more when compared with the case when small K_i . Even for large K_i , the amount of shrinking of the circle increases with an increase in N with all other parameters being fixed.

We can see that there might be some link between the eigenvalues of the superoperator, $M(U)$ and the underlying classical dynamics of the standard map. The degeneracies in the eigenvalues are affected by the value of K_i , which in the classical case controls the transition of the phase space from regular to mixed and finally to complete chaos. We do not yet know what the link exactly is. One can now ask various questions, such as - Is there anything special about purely real eigenvalues? How many real eigenvalues are present, and how does it vary with the parameters? What is the radius of the circle on which the eigenvalues lie? At what value of the parameter is there a transition from a circular region to an annular region? Are there eigenvalues that do not change as we vary N ?

Each of these questions is interesting and might lead to interesting connections between the spectral properties of the quantum channel and the underlying dynamics. We are trying to find answers to these questions. Some partial attempts are presented in the next part.

- **For different N :**

We have seen how the eigenvalue distribution changes with b and N . Next, we would like to see how the radius of the circle or the annular region changes with N . The eigenvalues distribution for $N = 10, 15$ and 20 for different b is illustrated in Fig. 6.16. For now, we restrict the analysis to the case when $K_1 = 0.1$ and $K_2 = 0.2$.

We can immediately observe a few things from fig.6.16. For $b = 0.05$ and $b = 0.1$, fig.6.16 (a) and (b), the radius of the circle is the same for the three values of N . But, as we increase b further to 0.5 , Fig. 6.16 (c), the radius of the circle is different for the three values of N . In fact, it decreases as we increase N , which is what we observed earlier, i.e., the extent to which the circle moves inside increases with increasing N for all other parameters being fixed. The circle corresponding to $N = 10$ encloses the circle for $N = 15$ and $N = 20$. There is still the line of real eigenvalues, and some real eigenvalues do lie outside the circle.

Now, as we increase b further to $1, 1.5$ or 2 as shown in Fig. 6.16 (d)-(f), we see that the circular regions for different N start to merge, and there is no clear boundary separating the eigenvalue distribution for the three cases.

Seeing the overlap between the eigenvalue distribution for $N = 10, 15$ and 20 , one might think that there are eigenvalues that are the same for $N = 10, 15$ and 20 . We are still working on this.

6.4 Relation Between Superoperator and Kraus Operators

We have seen different representations of Quantum Operations. But as they represent the same operations, we can always find the link between any two representations. The general quantum channel in terms of superoperator, M is -

$$M|\rho\rangle = |\rho'\rangle \quad (6.29)$$

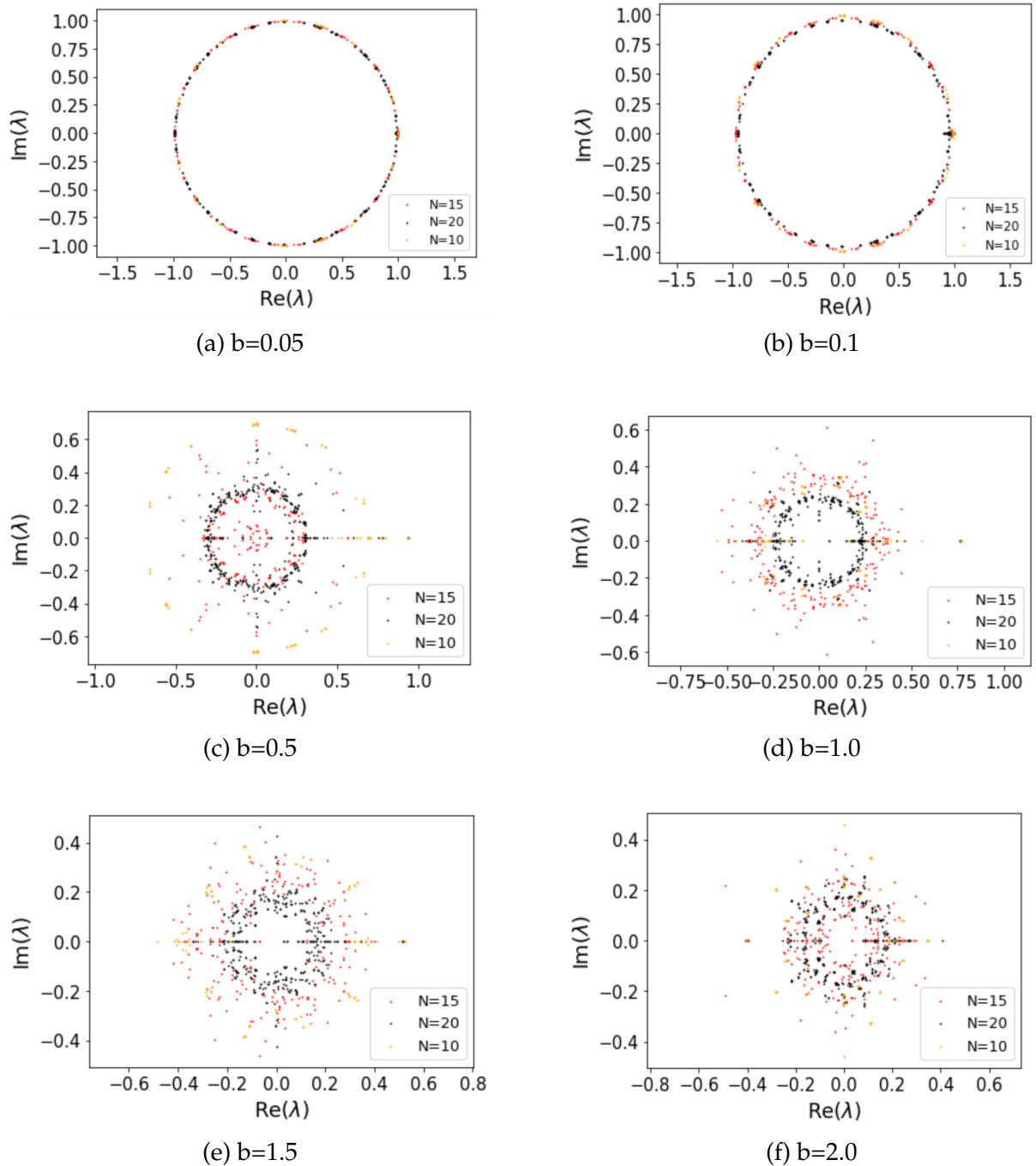


Figure 6.16: Eigenvalue distribution of M for $N=10,15,20$ with $K_1 = 0.1$ and $K_2 = 0.2$

Sudharshan, Mathews, and Rau in ref [31] introduced another matrix, the dynamical matrix, B , which is obtained by reshuffling(or, realignment) of matrix M .

$$B = M^{R_2} \quad (6.30)$$

Hence, in our case, B becomes-

$$B = \frac{1}{d} [U^{R_2} (U^{R_2})^\dagger] \quad (6.31)$$

In the review article [36], a relation between superoperator, M dynamical matrix, B and the Kraus operators has been presented. In Chapter 5, we have seen that the operator-sum representation of the quantum channel is given as -

$$\rho' = \sum_{\alpha} D_{\alpha} \rho D_{\alpha}^{\dagger} \quad (6.32)$$

the vectorization of the above equation gives -

$$|\rho'\rangle = \left(\sum_{\alpha} D_{\alpha} \otimes D_{\alpha}^* \right) |\rho\rangle \quad (6.33)$$

Comparing this with eq. 6.29 we get -

$$M = \sum_{\alpha} D_{\alpha} \otimes D_{\alpha}^* \quad (6.34)$$

Now, to get B , we need to reshuffle(or realign) M . The realignment of a tensor product between 2 operators is equal to the outer product of the vectorization of the operator. By doing that, we get,

$$B = \sum_{\alpha} |D_{\alpha}\rangle\langle D_{\alpha}| \quad (6.35)$$

The Kraus operators can be obtained by the matricized form of the eigenvectors of B . B is hermitian [31], and hence, we can write the spectral decomposition of B as -

$$B = \sum_{\alpha} \lambda_{\alpha} |\Lambda_{\alpha}\rangle\langle\Lambda_{\alpha}| \quad (6.36)$$

Thus,

$$D_{\alpha} = \sqrt{\lambda_{\alpha}} \text{mat}(|\Lambda_{\alpha}\rangle) \quad (6.37)$$

where $\text{mat}(.)$ represents the vectorized form of the vector.

Number of Kraus operators and Rank of B :

The Kraus operators obtained by diagonalizing the dynamical matrix, B , are called a canonical set of Kraus operators. A given quantum channel admits different Kraus representations operators,[30],[29]. The review article in ref [36] and also from the relation in eq. 6.37 it is clear that the number of Kraus operators in the canonical set is equal to the number of non-zero eigenvalues, which is also the rank of the dynamical matrix, B .

Bound on the rank of B for Standard Map:

B is a $N^2 \times N^2$ matrix where N is the local dimension of the system and environment. The maximum non-zero eigenvalues of B can be N^2 and thus, we can have a maximum of N^2 canonical set of Kraus operators.³ For the case when U is the unitary operator corresponding to the standard map,4.2.6 we have -

$$U = (U_1 \otimes U_2)U_b \quad (6.38)$$

where U_1 and U_2 are local unitaries to the system and environment, and U_b is a diagonal matrix that represents the interaction between the system and environment. Now, from eq. 6.31 we have -

$$B = \frac{1}{d} [(U_1 \otimes U_2)U_b]^{R_2} [((U_1 \otimes U_2)U_b)^{R_2}]^\dagger \quad (6.39)$$

This can be simplified using an identity mentioned in[5], which states-

$$((u_1 \otimes u_2)A(u_3 \otimes u_4))^{R_2} = (u_1 \otimes u_3^T)A^{R_2}(u_2^T \otimes u_4) \quad (6.40)$$

and hence, taking u_3 and u_4 as identity we can simplify eq. 6.39 to -

$$B = \frac{1}{d} [(U_1 \otimes I)U_b^{R_2}(U_b^{R_2})^\dagger(U_1^\dagger \otimes I)] \quad (6.41)$$

The rank of matrix B thus depends on the rank of the matrix, $U_b^{R_2}(U_b^{R_2})^\dagger$ because $U_1 \otimes I$ and $U_1^\dagger \otimes I$ are just some local unitary rotations.

We have seen in appendix B that U_b is a diagonal matrix, and it has N non-zero diagonal elements on reshuffling(R_2); we get a matrix with N non-zero entries and maximum it can have just N non-zero eigenvalues. Therefore, the maximum rank of the dynamical matrix

³We can still have other representations where the number of Kraus operators is larger than N^2 .

for this case can be N and not N^2 . Hence, the number of canonical sets of Kraus operators has an upper limit of N for a quantum channel corresponding to a quantum standard map.

We have come across some interesting results. But, have not answered the questions which we raised earlier. There seems to be a link between the eigenvalues of the quantum channel, $M(U)$ and the underlying classical dynamics associated with the unitary, U . We are still working on this and some future plans are mentioned in the next chapter.

Chapter 7

Summary and Future work

The "quantum signature of chaos" is one of the widely studied topics in the field of Quantum Chaos. The effect of the underlying classical dynamics on quantum energy eigenstates is known, and also we have reviewed a work, "Entangling Power of the Quantized Chaotic Systems"[\[25\]](#), which presented the connections of entanglement with chaos. In this work, the variation of entanglement entropy with chaos and how chaos maximizes the entropy is presented. Also, the scarring of quantum eigenstates by classical periodic orbit has been observed. Thus, the underlying classical dynamics have different effects in the quantum case depending on whether we are in a regular or chaotic regime in the classical case.

In sec.[4.4](#), we have seen that the entanglement entropy saturates as we increase the interaction; however, there are certain eigenstates of the unitary, U , which have low entanglement than most of the other eigenstates. These low entanglement states are the one that shows scarring phenomenon. These eigenstates are localized in the phase space; however, the states with entanglement near the saturation value are spread over the entire phase space. These are some of the "**quantum signatures of chaos**".

These results are for a coupled standard map that is closed and for which the dynamics in the quantum case are given by a unitary operator, U , discussed in [4.2.6](#). However, this no longer holds when there is interaction with the environment. The dynamics are no longer unitary. The transformation of the states is then given by a general quantum operation, which is a Quantum Channel. We can consider the second pendulum in the coupled system

as the environment, and now the interaction part of the unitary, U , is acting as a coupling strength of the system with the environment. The system is now an open single standard map whose dynamics are given by a channel, M (sec.5.2). The channel, M , is non-unitary for the non-zero value of b .

One can expect that there might be some effect on the underlying dynamics now on the channel, M . In order to observe such "quantum signatures of chaos" on the channel, M , we look at the spectral properties of the channel. There are various things one observes about the eigenvalue distribution of the channel, M (sec.6.3.3), as we vary various parameters. Some of which are -

- Eigenvalues are either purely real or complex, except in some cases, we get purely imaginary eigenvalues.
- The channel M is unital, and hence, we have one trivial largest eigenvalue, unity.
- All eigenstate converges to the eigenvector with eigenvalue 1, which is the maximally mixed state. The convergence to this maximally mixed state depends on the interaction strength between the system and the environment.
- Eigenvalues lie on the circle of radius less than unity for small b . And as we increase b , the circle shrinks and moves away from the unit circle. Also, for fixed b , the extent to which the circle shrinks depends on N . The extent of shrinking is more for larger N and fixed all other parameters.
- There is a line of purely real eigenvalues which grows as we increase either N or b .
- There is a transition from circular to ring for the eigenvalue distribution.
- For small K_i for which the classical standard map is nearly integrable, there are degeneracies in the eigenvalues, which get lifted for some eigenvalues as we increase K_i

The above observations show that there is some link between the eigenvalues of the map, M and the underlying classical dynamics. The link is not yet fully understood by us. There

is a line of real eigenvalues that may or may not have some link with the classical periodic orbit or "scarring", which, again, is not known to us. However, to gain some insight, we are at present looking at the husimi of the eigenvectors for some purely real and complex eigenvalues, which are still in progress and have not been presented here. On a side note, the study of spectral properties is important and can be linked with the correlation functions for dual unitary circuits[4]. The correlation functions are used for the study of ergodicity in the case of quantum chaos.

What lies ahead?

There are various directions where one can go from here. Some of our goals are -

- Finding the significance of the purely real eigenvalues and the corresponding eigenvectors associated with them, if any.
- Understanding the effect of underlying dynamics on the spectral properties of the channel, M .
- Building on the link between the channel, $M(U)$ and the eigenvectors of the unitary, U . The eigenvectors of the unitary, U , have entanglement entropy. Thus, we wish to find the link between the spectrum of the eigenvalue of M and the entanglement of the eigenvectors of unitary, U .
- Looking at the spectral properties of $M(U^t)$, where t is the time, and what does it signify?

We hope to get a better understanding of the theory explaining our observation. Chaos is an interesting and very complex phenomenon that is still not understood completely. We hope that we get a deeper understanding of a *glass of water* within the context of the complex and dynamic environment of the *Chaotic Sea!*

Appendix A

Proof of Schmidt Decomposition

Let us consider a pure bipartite system, $\mathcal{H}_d^A \otimes \mathcal{H}_d^B$. We are considering the case when A and B have the same local dimension, d. Any bipartite state can then be written as -

$$|\psi_{AB}\rangle = \sum_{i,j=1}^d c_{ij}|i_A\rangle|j_B\rangle \quad (\text{A.1})$$

where, $\{|i\rangle\}$ and $\{|j\rangle\}$ is some orthonormal bases for subsystem A and B. The above sum has d^2 elements as each i , and j goes from 1 to d .

Next, consider the matrix with elements as the coefficients, c_{ij} . Let C be the coefficient matrix which is a $(d \times d)$ array. The singular value decomposition of a square matrix, X , is given as -

$$X = RDS \quad (\text{A.2})$$

where R and S are unitary matrices, and D is a diagonal matrix and the diagonal elements are known as the singular values of X . Now, we can write the singular value decomposition of our coefficient matrix as -

$$C = U\sqrt{\Lambda}V \quad (\text{A.3})$$

Here, U , D and V are all $d \times d$ as A and B have the same local dimension Writing in element form, we get -

$$c_{ij} = \sum_{k=1}^d u_{ik}\sqrt{\lambda_k}v_{kj} \quad (\text{A.4})$$

Using this in eq. A.1 we get -

$$|\psi_{AB}\rangle = \sum_{i,j,k=1}^d u_{ik} \sqrt{\lambda_k} v_{kj} |i_A\rangle |j_B\rangle \quad (\text{A.5})$$

This can be rewritten as -

$$|\psi_{AB}\rangle = \sum_{k=1}^d \sqrt{\lambda_k} \left(\sum_{i=1}^d u_{ik} |i_A\rangle \right) \left(\sum_{j=1}^d v_{kj} |j_B\rangle \right) \quad (\text{A.6})$$

Thus, we get -

$$|\psi_{AB}\rangle = \sum_{k=1}^d \sqrt{\lambda_k} |k_A\rangle |k_B\rangle \quad (\text{A.7})$$

where, $|k_A\rangle = \sum_{i=1}^d u_{ik} |i_A\rangle$ and $|k_B\rangle = \sum_{j=1}^d v_{kj} |j_B\rangle$. The sum in eq. A.7 has d terms, and this is the power of Schmidt decomposition. We have gone from a sum with d^2 terms to a sum with just d -terms.

When the dimension of A and B are unequal, say, d_A and d_B respectively, then C is $d_A \times d_B$ matrix, U is $d_A \times d_A$, D is $d_A \times d_B$ and V is $d_B \times d_B$. Then it is easy to prove that the number of terms in the Schmidt decomposition will be the $\min\{d_A, d_B\}$.

Appendix B

Derivation of Unitary, U for Quantum Standard Map

The Hamiltonian¹ for kicked systems is of the form -

$$H = f(p) + V(q) \sum_{n=-\infty}^{\infty} \delta(t/T - n) \quad (\text{B.1})$$

where, $f(p)$ and $V(q)$ are operators and doesn't depend on time. To get the quantum map, we wish to result from the transformation relating the state, $|\psi\rangle$ after n^{th} and $(n+1)^{th}$. The Schrödinger equation for this system is given as -

$$i\hbar \frac{\partial}{\partial t} |\psi\rangle = f|\psi\rangle + V\delta_T \quad (\text{B.2})$$

where, δ_T represents the train of delta impulses. The time evolution of states in quantum mechanics is given by unitary operators. Let U be the operator which relates the state after n^{th} and $(n+1)^{th}$ kicks. The U would not depend on the kick number as the kicks are identical. Now, if $|\psi(n^+)\rangle$ is the state just after n^{th} kick then we have -

$$U|\psi(n^+)\rangle = |\psi(n+1^+)\rangle \quad (\text{B.3})$$

Let us consider the state just after n^{th} kick and just before $(n+1)^{th}$ kick, where the delta impulse is absent. In that case, the Hamiltonian is just, $H = f$ and we get -

$$|\psi(n+1^-)\rangle = \exp(-ifT/\hbar)|\psi(n^+)\rangle \quad (\text{B.4})$$

¹This derivation is presented in [7]. We are just reviewing the derivation.

The next task is to determine the change of state that happens suddenly at the instant of the kick. For that, consider an infinitesimally short time about the kick. During this short time, one can ignore the f part of Hamiltonian as kicking is dominated. Thus, the Schrödinger equation is then given as -

$$i\hbar \frac{\partial}{\partial t} |\psi\rangle = V\delta_T \quad (\text{B.5})$$

Integrating the above equation, we get -

$$|\psi(t')\rangle = \exp\left(-\frac{iV}{\hbar} \int_t^{t'} \delta_T dt\right) |\psi(t)\rangle \quad (\text{B.6})$$

here, $t = (n + 1)^-$ and $t' = (n + 1)^+$ Solving the integral is easy as we have a series of Dirac delta. Therefore, we get-

$$|\psi((n + 1)^+)\rangle = \exp(-iVT/\hbar) |\psi((n + 1)^-)\rangle \quad (\text{B.7})$$

Inserting Eq. B.4 in this we get -

$$|\psi(n + 1)\rangle = \exp(-iVT/\hbar) \exp(-ifT/\hbar) |\psi(n)\rangle \quad (\text{B.8})$$

This is the quantized version of the classical kicked map, and the unitary, U of the map is thus -

$$U = \exp(-iVT/\hbar) \exp(-ifT/\hbar) \quad (\text{B.9})$$

Translation Operators and Eigenvalues of position and momentum on a Torus: On a unit torus, q and p are restricted from 0 to 1, and this gives a finite-dimensional quantum space, unlike general position and momentum basis states which are infinite-dimensional.

Consider a N -dimensional Hilbert space. Let $|q_n\rangle$ and $|p_n\rangle$, $n = \{0, 1, 2, \dots, N - 1\}$ be the eigenstates of position and momentum. The translation operators in this finite-dimensional Hilbert space do not admit infinitesimal translations, which is the main distinction between a finite-dimensional and infinite-dimensional Hilbert space. The action of translation operators for the position and momentum eigenstates are then given as -

$$\langle q_n | T_q = \langle q_{n+1} |, \text{ and } \langle q_n | T_q^N = \langle q_{n+N} | \quad (\text{B.10})$$

and similarly,

$$T_p |p_n\rangle = |p_{n+1}\rangle, \text{ and } T_p^N |p_n\rangle = |p_{n+N}\rangle \quad (\text{B.11})$$

Just like in continuous quantum mechanics, the position and momentum basis are related by Fourier Transformation; we have for discrete quantum mechanics as -

$$|p_m\rangle = \frac{1}{\sqrt{N}} \sum_{n=0}^{N-1} \exp \left[\frac{2\pi i}{N} (n + \alpha)(m + \beta) \right] |q_n\rangle \quad (\text{B.12})$$

Now, if we act T_q on the above state we get -

$$T_q |p_m\rangle = \frac{1}{\sqrt{N}} \sum_{n=0}^{N-1} \exp \left[\frac{2\pi i}{N} (n + \alpha)(m + \beta) \right] T_q |q_n\rangle \quad (\text{B.13})$$

$$T_q |p_m\rangle = \frac{1}{\sqrt{N}} \sum_{n=0}^{N-1} \exp \left[\frac{2\pi i}{N} (n + \alpha)(m + \beta) \right] \exp \left[\frac{2\pi i}{N} (m + \beta) \right] |q_n\rangle \quad (\text{B.14})$$

where, $T_q |q_n\rangle = |q_{n+1}\rangle$, and we have used the fact that as we move along the position direction, the only change in the wavefunction is the phase.

Therefore,

$$T_q |p_m\rangle = \exp \left[\frac{2\pi i}{N} (m + \beta) \right] |p_m\rangle \quad (\text{B.15})$$

Therefore, the position translation operator is diagonal in momentum basis just like in continuous quantum mechanics and the positions eigenvalues are then given as -

$$p_m = \frac{m + \beta}{N} \quad (\text{B.16})$$

Similarly, one can show that the momentum translation operator is diagonal in the position basis, and the position eigenvalues are then given as -

$$q_n = \frac{n + \alpha}{N} \quad (\text{B.17})$$

α governs the parity symmetry in the system, and β governs the time-reversal symmetry, and they lie in the interval [0,1). We do not want to talk more about this as it will form a separate discussion in itself.

Matrix form of Unitary Operator, U for a Standard Map:

Now that we have determined the eigenvalue of position and position, the derivation of matrix U is just algebra. For a standard map, we have -

$$V = -\frac{K \cos(2\pi q)}{(2\pi)^2} \quad (\text{B.18})$$

$$f = \frac{p^2}{2} \quad (\text{B.19})$$

where, V , f , q and p are operators. Therefore, from eq. B.9 we get -

$$U = \exp\left[\frac{iK\cos(2\pi q)T}{(2\pi)^2\hbar}\right] \exp\left[\frac{-ip^2T}{2\hbar}\right] \quad (\text{B.20})$$

The number of states, N , is related to phase space volume as, $N=1/\hbar$. The matrix element in position basis is then given as -

$$\langle q'_n | U | q_n \rangle = \langle q'_n | \exp\left[\frac{-ip^2T}{2\hbar}\right] | q_n n \rangle \exp\left[\frac{iNK\cos(2\pi(n+\alpha))T}{(2\pi)^2}\right] \quad (\text{B.21})$$

Inserting momentum basis states in between and we get -

$$\langle q'_n | U | q_n \rangle = \sum_{m',m} \langle q'_n | p'_m \rangle \langle p'_m | \exp\left[\frac{-ip^2T}{2\hbar}\right] | p_m \rangle \langle p_m | q_n n \rangle \exp\left[\frac{iNK\cos(2\pi(n+\alpha))T}{(2\pi)^2}\right] \quad (\text{B.22})$$

and now using eq. B.12 we get -

$$U_{n'n} = \frac{1}{N} e^{\left(\frac{iNK}{2\pi} \cos(2\pi \frac{n+\alpha}{N})\right)} \sum_{m=0}^{N-1} e^{\left(-\pi i \left(\frac{(m+\beta)^2}{N}\right)\right)} e^{\left(\frac{2\pi i}{N} (m+\beta)(n-n')\right)} \quad (\text{B.23})$$

where we have taken the time period of kicking as one, $T=1$.

Appendix C

Completely Positivity of Quantum Channel using Kraus Operators.

The state of an open-quantum system evolves via a CPTP map, which in terms of Kraus operators, is given as-

$$\rho_{final} = \sum_i E_i \rho E_i^\dagger \quad (C.1)$$

For the input and output states being valid density-matrix, we have -

$$\sum_i E_i^\dagger E_i = I \quad (C.2)$$

This is also known as a trace-preserving channel. We can write $E_i \rho E_i^\dagger$ as-

$$E_i \rho E_i^\dagger = D_i D_i^\dagger \quad (C.3)$$

where, $D_i = E_i \sqrt{\rho}$. Since, $D_i D_i^\dagger$ is a positive operator, ρ_{final} is also a positive operator. Hence, the channel is positive. Now, if we consider an arbitrary extension, S' , to our system, S then we get -

$$(\mathcal{E}_S \otimes II) \rho_{SS'} = \sum_i (E_i \otimes I) \rho_{SS'} (E_i^\dagger \otimes I) \quad (C.4)$$

Each of the terms in the sum is positive; thus, the entire sum is positive. Therefore,

$$(\mathcal{E}_S \otimes II) \geq 0 \quad (C.5)$$

This gives the complete positivity condition of the channel.

Appendix D

Realignment and Partial Transpose Operation. Also deriving M and M_c

For a bipartite system, we can define certain operations on the operators. The operations which we are looking at are realignment and partial transpose. Let A be a bipartite operator. The matrix element of A is then given as -

$$A_{i\alpha,j\beta} = \langle i\alpha|A|j\beta\rangle \quad (\text{D.1})$$

The realignment and partial transpose operation can then be defined as-

- **Realignment Operation:** Realignment operation is a kind of reshuffling of elements of the matrix. We can have-

$$A_{\beta\alpha,ji}^{R_1} = \langle \beta\alpha|A^{R_1}|ji\rangle \quad (\text{D.2})$$

and,

$$A_{ij\alpha\beta}^{R_2} = \langle ij|A^{R_2}|\alpha\beta\rangle \quad (\text{D.3})$$

- **Partial Transpose** Partial transpose is nothing but the transpose operation in one of the subsystems only. We can define T_1 and T_2 corresponding to the transpose of subsystems 1 and 2, respectively. It is given as -

$$A_{i\beta,j\alpha}^{T_1} = \langle i\beta|A^{T_1}|j\alpha\rangle \quad (\text{D.4})$$

and,

$$A_{j\alpha,i\beta}^{T_2} = \langle j\alpha|A^{T_2}|i\beta\rangle \quad (\text{D.5})$$

Deriving the expression of channel, M and its complementary, M_c :

Let us consider a system and an environment, which together form a closed system. Let ρ_{SE} be the density matrix for this system. Let the initial state ρ_{SE} be unentangled and is product form. Let ρ_S and ρ_E be the state of the system and environment, respectively. Without loss of generality, we can see the initial state of the environment, ρ_E as a maximally mixed state, I/d . We can then find the state of the system after a quantum operation as -

$$\rho'_S = Tr_E [U^\dagger (\rho_S \otimes I/d) U] \quad (D.6)$$

here, U is unitary as it acts on the system and environment, which is a closed system.

Writing the element form of this equation, we get-

$$\langle j | \rho'_S | i \rangle = \sum_{\alpha} \langle j\alpha | U^\dagger (\rho_S \otimes I/d) U | i\alpha \rangle \quad (D.7)$$

Due to the freedom one gets from completeness relation, we can insert a complete basis set as shown below-

$$\langle j | \rho'_S | i \rangle = \sum_{\alpha, k, l, \gamma, \gamma'} \langle j\alpha | U^\dagger | l\gamma' \rangle \langle l\gamma' | (\rho_S \otimes I/d) | k\gamma \rangle \langle k\gamma | U | i\alpha \rangle \quad (D.8)$$

As the second subsystem state is just I/d , we get -

$$\langle j | \rho'_S | i \rangle = \frac{1}{d} \sum_{\alpha, k, l, \gamma, \gamma'} \langle j\alpha | U^\dagger | l\gamma' \rangle \langle l | (\rho_S | k \rangle \langle k\gamma | U | j\alpha \rangle \delta_{\gamma, \gamma'} \quad (D.9)$$

where, $\langle l\gamma' | (\rho_S \otimes I/d) | k\gamma \rangle = \langle l | \rho_S | k \rangle \langle \gamma | I/d | \gamma' \rangle = \frac{1}{d} \langle l | \rho_S | k \rangle \delta_{\gamma, \gamma'}$

Doing the realignment operations in eq. D.9 we get -

$$\langle j | \rho'_S | i \rangle = \frac{1}{d} \sum_{\alpha, k, l, \gamma} \langle \gamma\alpha | (U^\dagger)^{R_1} | lj \rangle \langle ki | U^{R_2} | \gamma\alpha \rangle \langle l | (\rho_S | k \rangle \quad (D.10)$$

Using the identity, $(U^\dagger)^{R_1} = (U^{R_2})^\dagger$ and summing over α and γ , we get-

$$\langle j | \rho'_S | i \rangle = \frac{1}{d} \sum_{k, l} \langle ki | U^{R_2} (U^{R_2})^\dagger | lj \rangle \langle l | (\rho_S | k \rangle \quad (D.11)$$

If we define, the vectorization of an operator as -

$$\langle l | (\rho_S | k \rangle = \langle lk | \rho_S \rangle \quad (D.12)$$

then, eq. D.11 becomes -

$$\langle ji|\rho'_S\rangle = \frac{1}{d} \sum_{k,l} \langle ji| [U^{R_2}(U^{R_2})^\dagger]^{R_1} |lk\rangle \langle lk|(\rho_S) \quad (\text{D.13})$$

Therefore, we can rewrite this in terms of channel, M as -

$$|\rho'_S\rangle = M|\rho_S\rangle \quad (\text{D.14})$$

where, $|\rho_S\rangle = \langle lk|\rho_S\rangle$ and M is given as -

$$M = \frac{1}{d} [U^{R_2}(U^{R_2})^\dagger]^{R_1} \quad (\text{D.15})$$

The Complementary Channel, M_c :

The complementary channel, M_c is defined as -

$$M_c = M(SU) \quad (\text{D.16})$$

where, S is a swap operator, given as -

$$S|\phi_A\rangle|\phi_B\rangle = |\phi_B\rangle|\phi_A\rangle \quad (\text{D.17})$$

From comparing with eq. D.6 we then have -

$$\langle \alpha|\rho''_S|\beta\rangle = \sum_i \langle i\alpha|U^\dagger S(I_E/d \otimes \rho_S)SU|i\beta\rangle \quad (\text{D.18})$$

We can now insert four complete sets of basis to get -

$$\langle \alpha|\rho''_S|\beta\rangle = \sum_{i,k,\gamma,l,\gamma',n,m,\delta,\delta'} \langle i\alpha|U^\dagger|k\gamma\rangle \langle k\gamma|S|m\delta\rangle \langle m\delta(I_E/d \otimes \rho_S)|n\delta'\rangle \langle n\delta'|S|l\gamma'\rangle \langle l\gamma'|U|i\beta\rangle \quad (\text{D.19})$$

The swap, S operation is given as - $\langle k\gamma|S|m\delta\rangle = \delta_{\delta,k}\delta_{m,\gamma}$

Using this, we get -

$$\langle \alpha|\rho''_S|\beta\rangle = \frac{1}{d} \sum_{i,k,l,\gamma} \langle i\alpha|U^\dagger|k\gamma\rangle \langle k|\rho_S|l\rangle \langle l\gamma|U|i\beta\rangle \quad (\text{D.20})$$

Now, doing partial transpose operations, we get -

$$\langle \alpha|\rho''_S|\beta\rangle = \frac{1}{d} \sum_{i,k,l,\gamma} \langle i\gamma|(U^{T_2})^\dagger|k\alpha\rangle \langle l\beta|U^{T_2}|i\gamma\rangle \langle k|\rho_S|l\rangle \quad (\text{D.21})$$

Summing over i and γ we get -

$$\langle \alpha | \rho''_S | \beta \rangle = \frac{1}{d} \sum_{k,l} \langle l\beta | U^{T_2} | (U^{T_2})^\dagger | k\alpha \rangle \langle k | \rho_S | l \rangle \quad (\text{D.22})$$

which on further realignment operation gives -

$$\langle \alpha | \rho''_S | \beta \rangle = \frac{1}{d} \sum_{k,l} \langle \alpha\beta | [U^{T_2} | (U^{T_2})^\dagger]^{R_1} | kl \rangle \langle k | \rho_S | l \rangle \quad (\text{D.23})$$

Again by vectorization, we get-

$$|\rho''_S\rangle = M_c |\rho_S\rangle \quad (\text{D.24})$$

where, M_c is given as -

$$M = \frac{1}{d} [U^{T_2} (U^{T_2})^\dagger]^{R_1} \quad (\text{D.25})$$

Bibliography

- [1] Eric J Heller, Patrick W O'Connor, and John Gehlen. "The eigenfunctions of classically chaotic systems". In: *Physica Scripta* 40.3 (1989), p. 354. DOI: [10.1088/0031-8949/40/3/017](https://doi.org/10.1088/0031-8949/40/3/017). URL: <https://dx.doi.org/10.1088/0031-8949/40/3/017>.
- [2] Robert Devaney. *An Introduction to Chaotic Dynamical Systems*. Oct. 2021. ISBN: 9780429280801. DOI: [10.1201/9780429280801](https://doi.org/10.1201/9780429280801).
- [3] Steven H. Strogatz. *Nonlinear Dynamics and Chaos: With Applications to Physics, Biology, Chemistry, and Engineering*. CRC Press, 2018.
- [4] Bruno Bertini, Pavel Kos, and Tomaž Prosen. "Exact Correlation Functions for Dual-Unitary Lattice Models in 1+1 Dimensions". In: *Phys. Rev. Lett.* 123 (21 2019), p. 210601. DOI: [10.1103/PhysRevLett.123.210601](https://doi.org/10.1103/PhysRevLett.123.210601). URL: <https://link.aps.org/doi/10.1103/PhysRevLett.123.210601>.
- [5] S. Aravinda, Suhail Ahmad Rather, and Arul Lakshminarayan. "From dual-unitary to quantum Bernoulli circuits: Role of the entangling power in constructing a quantum ergodic hierarchy". In: *Phys. Rev. Res.* 3 (4 2021), p. 043034. DOI: [10.1103/PhysRevResearch.3.043034](https://doi.org/10.1103/PhysRevResearch.3.043034). URL: <https://link.aps.org/doi/10.1103/PhysRevResearch.3.043034>.
- [6] V.I.Arnold. "Mathemactical Methods in Classical Mechanics". In: (1978). URL: <https://link.springer.com/book/10.1007/978-1-4757-2063-1>.
- [7] Arul Lakshminarayan. "Classical and quantum Chaos plus RMT and some applications." In: (). URL: <https://drive.google.com/file/d/1Yw34qGJUcqfeMbIHs5HC6zvlpKsf5nvp/view>.
- [8] H. Poincaré. *Les méthodes nouvelles de la mécanique céleste*. Vol. 1. Gauthier-Villars, 1892.
- [9] E. Ott. *Chaos in Dynamical Systems*. Cambridge University Press, 1993.
- [10] S. H. Strogatz. *Nonlinear Dynamics and Chaos: with Applications to Physics, Biology, Chemistry, and Engineering*. Addison-Wesley, 1994.
- [11] B. V. Chirikov. "A universal instability of many-dimensional oscillator systems". In: *Physics Reports* 52.5 (1979), pp. 263–379. DOI: [10.1016/0370-1573\(79\)90023-1](https://doi.org/10.1016/0370-1573(79)90023-1). URL: [https://doi.org/10.1016/0370-1573\(79\)90023-1](https://doi.org/10.1016/0370-1573(79)90023-1).

- [12] B. V. Chirikov. *Research concerning the theory of nonlinear resonances and absorption of particle accelerators*. Tech. rep. Dubna, Russia: Joint Institute for Nuclear Research, 1960.
- [13] R.S. MacKay. "A renormalization approach to invariant circles in area-preserving maps". In: *Physica D: Nonlinear Phenomena* 7.1 (1983), pp. 283–300. ISSN: 0167-2789. DOI: [https://doi.org/10.1016/0167-2789\(83\)90131-8](https://doi.org/10.1016/0167-2789(83)90131-8). URL: <https://www.sciencedirect.com/science/article/pii/0167278983901318>.
- [14] D F Escande. "Large-Scale Stochasticity in Hamiltonian Systems". In: *Physica Scripta* 1982.T2A (1982), p. 126. DOI: [10.1088/0031-8949/1982/T2A/016](https://doi.org/10.1088/0031-8949/1982/T2A/016). URL: <https://dx.doi.org/10.1088/0031-8949/1982/T2A/016>.
- [15] Claude Froeschle. "On the Number of Isolating Integrals in Systems with Three Degrees of Freedom (Papers appear in the Proceedings of IAU Colloquium No. 10 Gravitational N-Body Problem (ed. by Myron Lecar), R. Reidel Publ. Co., Dordrecht-Holland.)" In: 14.1 (Nov. 1971), pp. 110–117. DOI: [10.1007/BF00649198](https://doi.org/10.1007/BF00649198).
- [16] Michael A. Nielsen and Isaac L. Chuang. *Quantum Computation and Quantum Information*. 10th Anniversary edition. Cambridge: Cambridge University Press, 2010. DOI: [10.1017/CBO9780511976667](https://doi.org/10.1017/CBO9780511976667).
- [17] Martin C. Gutzwiller. "Periodic Orbits and Classical Quantization Conditions". In: *Journal of Mathematical Physics* 12 (1971), pp. 343–358.
- [18] Michael Berry. "Quantum chaology, not quantum chaos". In: *Physica Scripta* 40.3 (1989), p. 335. DOI: [10.1088/0031-8949/40/3/013](https://doi.org/10.1088/0031-8949/40/3/013). URL: <https://dx.doi.org/10.1088/0031-8949/40/3/013>.
- [19] G Casati and I Guarneri. "Quantum chaos and quantum computers". In: *Physica D: Nonlinear Phenomena* 19.1-2 (1986), pp. 277–284.
- [20] Giulio Casati et al. "Stochastic behavior of a quantum pendulum under a periodic perturbation". In: vol. 93. Apr. 2006, pp. 334–352. ISBN: 3-540-09120-3. DOI: [10.1007/BFb0021757](https://doi.org/10.1007/BFb0021757).
- [21] N.L. Balazs and A. Voros. "The quantized Baker's transformation". In: *Annals of Physics* 190.1 (1989), pp. 1–31. ISSN: 0003-4916. DOI: [https://doi.org/10.1016/0003-4916\(89\)90259-5](https://doi.org/10.1016/0003-4916(89)90259-5). URL: <https://www.sciencedirect.com/science/article/pii/0003491689902595>.
- [22] M.V Berry et al. "Quantum maps". In: *Annals of Physics* 122.1 (1979), pp. 26–63. ISSN: 0003-4916. DOI: [https://doi.org/10.1016/0003-4916\(79\)90296-3](https://doi.org/10.1016/0003-4916(79)90296-3). URL: <https://www.sciencedirect.com/science/article/pii/0003491679902963>.
- [23] M Saraceno. "Classical structures in the quantized baker transformation". In: *Annals of Physics* 199.1 (1990), pp. 37–60. ISSN: 0003-4916. DOI: [https://doi.org/10.1016/0003-4916\(90\)90367-W](https://doi.org/10.1016/0003-4916(90)90367-W). URL: <https://www.sciencedirect.com/science/article/pii/000349169090367W>.

- [24] K. Furuya, M. C. Nemes, and G. Q. Pellegrino. "Quantum Dynamical Manifestation of Chaotic Behavior in the Process of Entanglement". In: *Phys. Rev. Lett.* 80 (25 1998), pp. 5524–5527. DOI: [10.1103/PhysRevLett.80.5524](https://doi.org/10.1103/PhysRevLett.80.5524). URL: <https://link.aps.org/doi/10.1103/PhysRevLett.80.5524>.
- [25] Arul Lakshminarayan. "Entangling power of quantized chaotic systems". In: *Physical Review E* 64.3 (2001). DOI: [10.1103/physreve.64.036207](https://doi.org/10.1103/physreve.64.036207). URL: <https://doi.org/10.1103>.
- [26] Thomas Guhr, Axel Müller-Groeling, and Hans A. Weidenmüller. "Random-matrix theories in quantum physics: common concepts". In: *Physics Reports* 299.4-6 (1998), pp. 189–425. DOI: [10.1016/s0370-1573\(97\)00088-4](https://doi.org/10.1016/s0370-1573(97)00088-4). URL: <https://doi.org/10.1016>.
- [27] I.I. Gurevich and M.I. Pevsner. "Repulsion of nuclear levels". In: *Nuclear Physics* 2.5 (1956), pp. 575–581. ISSN: 0029-5582. DOI: [https://doi.org/10.1016/0029-5582\(57\)90069-X](https://doi.org/10.1016/0029-5582(57)90069-X). URL: <https://www.sciencedirect.com/science/article/pii/002955825790069X>.
- [28] M. S. Santhanam, V. B. Sheorey, and Arul Lakshminarayan. "Effect of classical bifurcations on the quantum entanglement of two coupled quartic oscillators". In: *Physical Review E* 77.2 (2008). DOI: [10.1103/physreve.77.026213](https://doi.org/10.1103/physreve.77.026213). URL: <https://doi.org/10.1103>.
- [29] Michael A. Nielsen and Isaac L. Chuang. *Quantum Computation and Quantum Information*. Cambridge University Press, 2010. URL: <https://csis.pace.edu/~ctappert/cs837-19spring/QC-textbook.pdf>.
- [30] Karl Kraus. *States, Effects, and Operations: Fundamental Notions of Quantum Theory*. Berlin, Germany: Springer-Verlag, 1983.
- [31] E. C. G. Sudarshan, P. M. Mathews, and Jayaseetha Rau. "Stochastic Dynamics of Quantum-Mechanical Systems". In: *Phys. Rev.* 121 (3 1961), pp. 920–924. DOI: [10.1103/PhysRev.121.920](https://doi.org/10.1103/PhysRev.121.920). URL: <https://link.aps.org/doi/10.1103/PhysRev.121.920>.
- [32] Michael M. Wolf. "Quantum Channels and Operations - A guided tour." In: (2012). URL: <https://mediatum.ub.tum.de/doc/1701036/document.pdf>.
- [33] Wojciech Bruzda et al. "Universality of spectra for interacting quantum chaotic systems". In: *Physical Review E* 81.6 (2010). DOI: [10.1103/physreve.81.066209](https://doi.org/10.1103/physreve.81.066209). URL: <https://doi.org/10.1103>.
- [34] Padraig Bartlett. "Lecture notes: The Schur Decomposition". In: (). URL: http://web.math.ucsb.edu/~padraig/ucsb_2013_14/math108b_w2014/math108b_w2014_lecture5.pdf.
- [35] Wojciech Bruzda et al. "Random quantum operations". In: *Physics Letters A* 373.3 (2009), pp. 320–324. DOI: [10.1016/j.physleta.2008.11.043](https://doi.org/10.1016/j.physleta.2008.11.043). URL: <https://doi.org/10.1016>.

- [36] Vinayak Jagadish and Francesco Petruccione. “An Invitation to Quantum Channels”. In: *Quanta* 7.1 (2018), p. 54. DOI: [10.12743/quanta.v7i1.77](https://doi.org/10.12743/quanta.v7i1.77). URL: <https://doi.org/10.12743>.